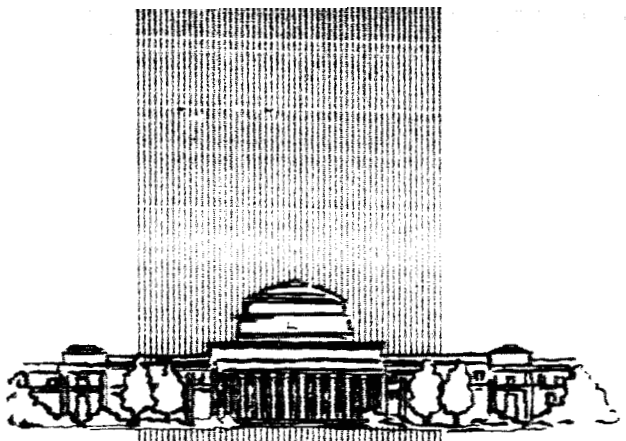

# MASSACHUSETTS INSTITUTE OF TECHNOLOGY

TE-10

## A CRYOGENIC TEST-MASS SUSPENSION FOR A SENSITIVE ACCELEROMETER

by

Philip Kenyon Chapman

June 1964

Degree of Master of Science



EXPERIMENTAL ASTRONOMY LABORATORY
MASSACHUSETTS INSTITUTE OF TECHNOLOGY
CAMBRIDGE 39, MASSACHUSETTS

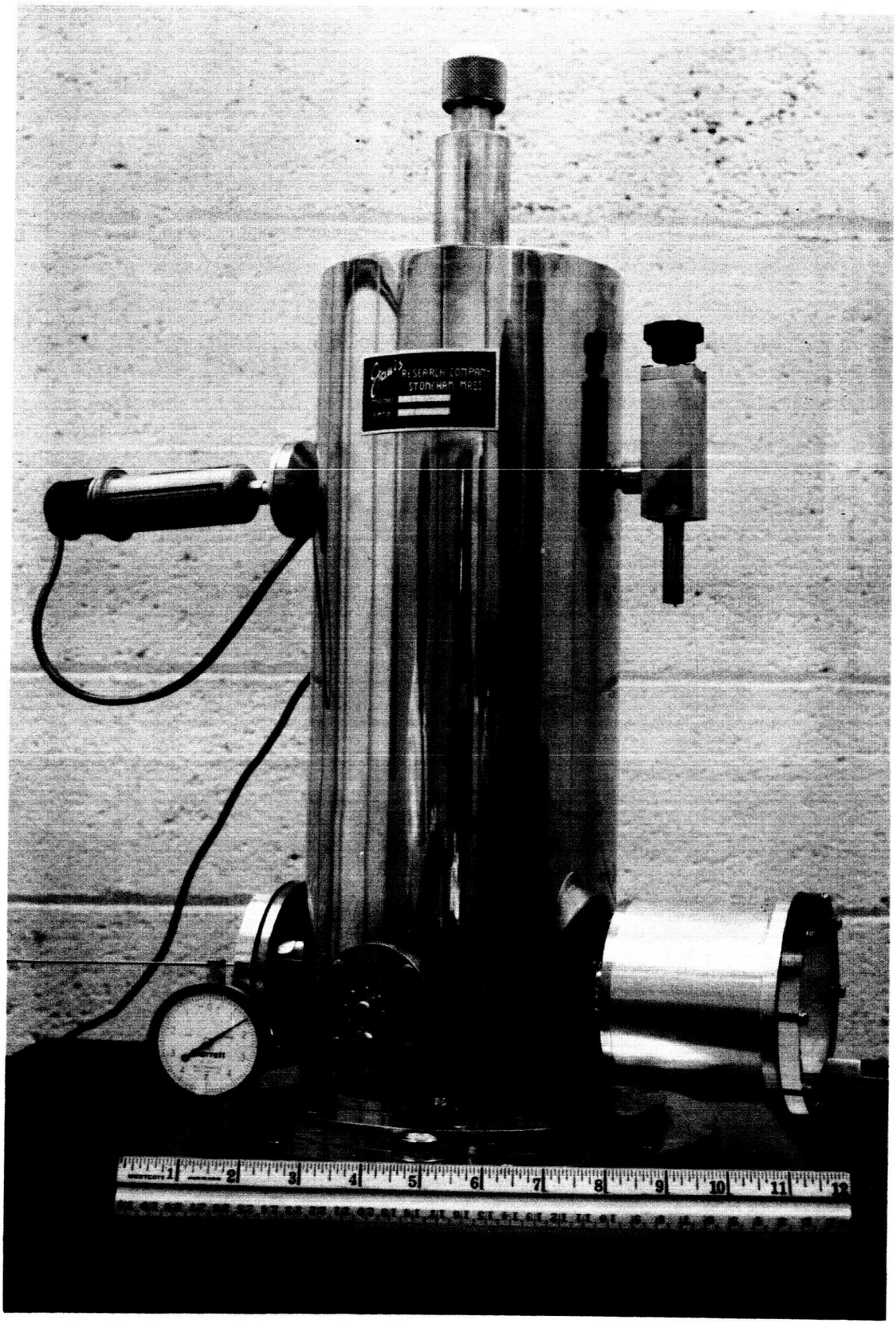
RESEARCH COMPANY
STONEHAM MASS

# A CRYOGENIC TEST-MASS SUSPENSION FOR A SENSITIVE ACCELEROMETER

by

PHILIP KENYON CHAPMAN

B. Sc., Sydney University

(1956)

SUBMITTED IN PARTIAL FULFILLMENT

OF THE REQUIREMENTS FOR THE

DEGREE OF MASTER OF SCIENCE

at the

MASSACHUSETTS INSTITUTE OF TECHNOLOGY

June, 1964

Signature of Author P. K. Chapman

Department of Aeronautics and Astronautics, June 1964

Certified by Robert L. Mueller

Thesis Supervisor

Accepted by Judson R. Baron

Chairman, Departmental Graduate Committee

# A CRYOGENIC TEST-MASS SUSPENSION FOR A SENSITIVE ACCELEROMETER

by

Philip K. Chapman

Submitted to the Department of Aeronautics and Astronautics on May 22, 1964, in partial fulfillment of the requirements for the degree of Master of Science.

## ABSTRACT

LLAMA (for Low-Level Acceleration Measurement Apparatus) is an investigation of techniques for the measurement of acceleration in the range below $10^{-6}$g. The design choices for the various components of an experimental accelerometer are briefly outlined, the main emphasis being on methods of supporting the test-mass. Factors affecting the design of a superconducting (Meissner Effect) test-mass suspension are discussed in some detail, and the construction of a feasibility demonstration model is described. The results of tests of the experimental instrument are presented, the conclusion being that the system shows promise of quite exceptional sensitivity, which should be realized when the other components have been assembled. Finally, several modifications are suggested which may allow operation down to at least $10^{-10}$g.

Thesis Supervisor: Robert K. Mueller

Title: Associate Professor of Aeronautics and Astronautics

## ACKNOWLEDGEMENTS

The author wishes to express his appreciation to the following persons: Professor R.K. Mueller, for his patience during this rather protracted investigation; Mr Shaoul Ezekiel, for his close collaboration in all phases of the project; Professor W.R. Markey, Mr Thomas Egan and Mr Richard Jankins of the Experimental Astronomy Laboratory, without whose cooperation the experiments would have been impossible; and Professor S.C. Collins and Mr Robert Cavileer of the Cryogenic Engineering Laboratory, for their advice and their tireless ministering to LLAMA's thirst for liquid helium.

This research was carried out under DSR Contract 5007, sponsored by NASA under Grant Number NsG 254-62.

# TABLE OF CONTENTS

TABLE OF CONTENTS (CONTINUED)

# ILLUSTRATIONS

Frontispiece: The LLAMA Suspension Dewar

# CHAPTER I

# INTRODUCTION

## 1.1 Applications of Very Sensitive Accelerometers

At the present time, devices are available for the reliable measurement of acceleration down to about $10^{-6}$g. Sensitivities approaching $10^{-9}$g have on occasion been claimed, but the calibration and stability of such instruments is open to serious question.

The development of a capability of making routine acceleration measurements in the micron/sec$^2$ ($10^{-7}$g) range and below would be useful in a number of areas, for instance:

i) Inertial guidance of electrically propelled space vehicles. This requires threshold sensitivities of about $10^{-7}$g.

ii) Microseismology, including the detection of remote explosions. The accelerations of interest are of the order of $10^{-8}$g, with periods of 1-100 seconds[1].

iii) The levelling of test tables during the precise test and calibration of other inertial components and the establishment of statistical models for the errors in such components.

iv) Vertical indication in orbit by active tracking of the gravity gradient. Thresholds below $10^{-10}$g are required[2].

v) Various important physical experiments, such as tests of the principle of equivalence and the detection of gravitational waves[3].

## 1.2 The LLAMA Concept

LLAMA (for Low Level Acceleration Measurement Apparatus) is a system which is presently under development in the Experimental Astronomy Laboratory of the Massachusetts Institute of Technology. The object of this program is the investigation of techniques for the construction of an accelerometer with a threshold sensitivity well below $10^{-6}$g. While the present system is intended for laboratory use only, it is hoped that the technology developed will be of use in constructing operational accelerometers.

The first application of the system under development will be as a sensor for use in the dynamic levelling of an inertial test table: i.e., a component of an active filter of microseismic disturbances.

In a terrestrial calibration facility, it is extremely difficult to produce known accelerations of the magnitude of interest here. As an example, tilting a test table from the horizontal through one arc second gives an acceleration component parallel to the table of 5 μg. For this reason, a primary design consideration in the present program was that the system should be absolute in the sense that it did not require calibration in terms of a known acceleration input.

The simplest form of accelerometer consists of a damped, elastically suspended test-mass, with some form of readout of the displacement of the mass under an applied acceleration. For single

axis operation, the test-mass must be supported, in directions perpendicular to the sensitive axis, by means of forces which are essentially decoupled from the sensitive axis.

Figure 1 is a diagram showing the various components of this type of accelerometer, in an elementary form. As mentioned above, a suitable calibration system (shown schematically by the balance pan and weights at the right in the figure) is of fundamental importance if the instrument is to be of use at very low acceleration levels.

The design approach used in the LLAMA program is to take each component of a simple accelerometer of this type and seek a new mechanization which will substantially improve performance. Chapter II contains a brief survey of the considerations involved in the design and of the system concept which resulted. The rest of this report is devoted to the detailed design of the test mass support and to the evaluation of an experimental model.

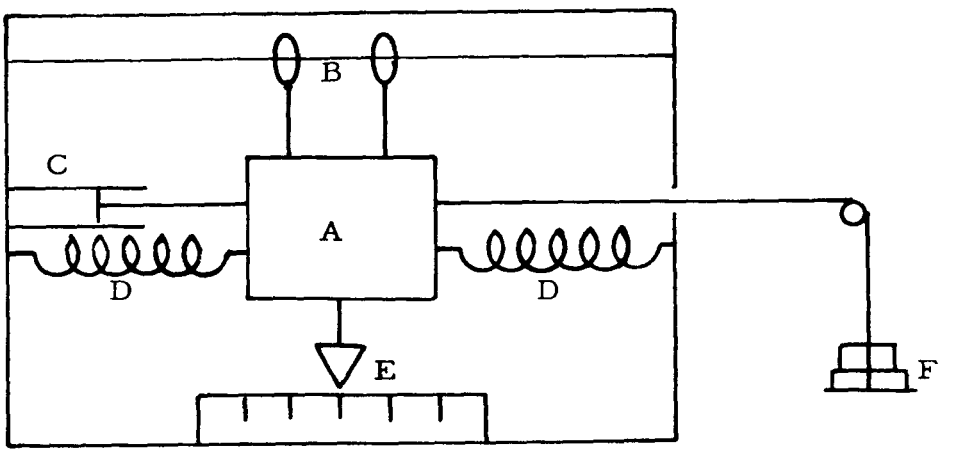


A: Test-Mass
B: Test-Mass Suspension
C: Damping
D: Restoring Force Generator
E: Displacement Readout
F: Calibration

Figure 1: An Elementary Accelerometer

# CHAPTER II

# SYSTEM DESIGN

## 2.1 General Design Considerations

It is a relatively simple matter to design a very sensitive accelerometer for use under free-fall conditions, as long as it is also possible to conduct any required test and calibration of the instrument under zero-gravity conditions. For a laboratory system, however, it is necessary to support the test-mass in the gravitational field of the Earth: as it is hardly possible that one could devise a support system with an adequate vertical stability, this implies that the instrument should be sensitive to horizontal acceleration only.

Microseisms constitute a background noise in all terrestrial acceleration measurements. Typically, the peak activity in the horizontal plane consists of a vibration with an amplitude of a few microns and periods of the order of a few seconds, giving rms accelerations of about $10^{-7}$g. Because of this problem, the initial LLAMA system is being designed for operation in the vicinity of $10^{-6}$g, so as to check the feasibility of the techniques used without undue complication of the test apparatus. The instrument is, however, theoretically capable of operation at much lower levels.

## 2.2 Support of the Test-Mass

The primary goal in the design of a test-mass suspension for an accelerometer is control of the interaction between support forces and the dynamics along the sensitive axis. In general, the following types of force-coupling may occur:

i) Threshold effects, static friction, etc. Any threshold which is present clearly imposes a lower limit on the attainable sensitivity of the instrument. For the purposes of LLAMA, such effects must be kept below $10^{-9}$ dynes, if at all possible.

ii) Conservative (position-dependent) forces: Assuming that no sharp non-linearities (e.g., mechanical hysteresis) are present, the level of force of this type which is acceptable depends on the expected amplitude of displacement. For instance, if the displacement is kept within 1 micron of the null position, an initial 'spring constant' due to the suspension of 0.1 dynes/cm would allow operation at least down to the $10^{-6}$g range. For high sensitivity of the instrument, a trade-off must be made between the difficulty of providing low conservative forces along the sensitive axis and the difficulty of detecting very small displacements.

iii) Dissipative (velocity-dependent) forces: It is of course essential that any motion of the test-mass in directions other than the sensitive axis be reasonably well damped. A small amount of natural damping of motion along the sensitive axis is also acceptable, although a fixed time constant means that the test-mass will be more than critically damped at sufficiently low acceleration levels.

For the present purposes, force-coupling corresponding to higher time derivatives of the test-mass displacement may be ignored.

Because almost any conceivable mechanical suspension would exhibit threshold and/or hysteretic effects beyond the stringent LLAMA tolerances, it was decided that some form of electromagnetic suspension would be used.

### 2.2.1 Magnetic Suspension

It can be shown quite generally that no configuration of permanent magnets is capable of stably supporting a magnetised test mass (Earnshaw's theorem). However, a ferromagnetic object may be suspended in a magnetic field if the field intensity be controlled by feedback from the position of the object. This principle has been used[4] to suspend models in wind tunnels, so as to avoid interference from support structures.

This technique is quite complex and expensive, and it is difficult to create sufficient spatial homogeneity of the fields along the sensitive axis for use in a low-level accelerometer.

A variant of this method is the magnetic resonant suspension[5] commonly used in floated inertial instruments. While avoiding the complexities of suspension feedback loops, this system suffers from the same type of field homogeneity problem, and in addition it is difficult to damp oscillations in directions other than the sensitive axis.

### 2.2.2 Electric Suspension

The electrically suspended gyro (ESG) demonstrates the feasibility of this type of support for inertial instruments[6]. For use in an accelerometer, a typical design is shown in Figure 2. A light conducting cylinder of radius a, constituting the test-mass, is contained within an outer electrode cylinder of radius b. The outer cylinder consists of four electrodes, numbered 1 to 4 in the figure.

Application of a voltage between any adjacent pair of electrodes produces a stress at the surface of the test-mass which is given by $0.442\ E^2$ microdynes/$cm^2$, where E is the voltage gradient at the surface in volts/cm, attracting the float to the excited electrodes. It is clear that, in order to support a float of reasonable weight in the Earth's gravitational field, quite high voltage gradients are required. The clearances around the float must therefore be very small, of the order of 25 microns, and the system must operate in a high vacuum ($10^{-8}$ torr or better) so as to prevent electrical flashover.

As in the case of the magnetic suspension, this device is inherently unstable: the float height must be stabilized by feedback techniques. A convenient error signal may be obtained by comparing the capacitance between one pair of adjacent electrodes with that of the opposite pair in a high frequency bridge. For horizontal and vertical stabilization, two servo loops are of course required.

A resonant suspension technique is also possible in this case, the main disadvantage being the difficulty of providing adequate damping.

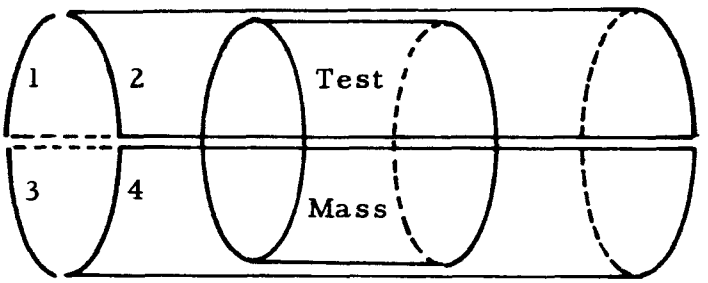


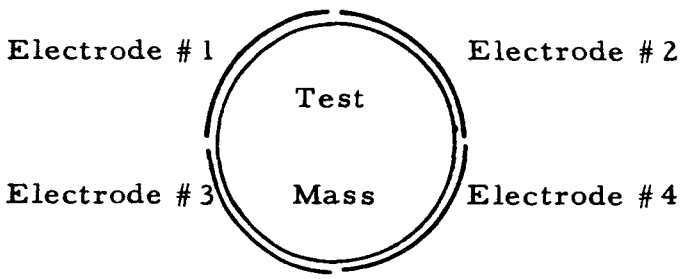


Figure 2: Geometry for Electric Test-Mass Suspension

The dissipative forces in this type of suspension are extremely low, being mainly due to drag from residual gas in the system. If the outer cylinder be sufficiently long, so that end effects may be ignored, the only source of axial conservative forces is geometrical imperfection of the electrode and float cylinders. In particular, because of the very small separation between the float and the electrodes, surface roughness may produce axial forces which are significant at the levels under consideration for LLAMA.

While electric suspension is quite attractive (especially for use in the space environment, where the low support forces required allow much larger clearances), rather elaborate facilities are needed in order to construct the device. In the first place, the float should have as low a density as possible; beryllium is the usual choice, despite the machining problems introduced. Secondly, the tight dimensional tolerances make a pressurized clean room mandatory for construction.

### 2.2.3 Charged-Particle Suspension

In the electric suspension systems described above, the test-mass carries no net charge, the support forces being generated by polarization of the float under an applied electric field. It is also possible to support a charged particle in an electric field[7], if some provision be made so that the charge does not leak away too rapidly.

Apart from the difficulty of adequate position detection, support of a charged particle by servo control of an applied electric field is a relatively simple matter. A more interesting possibility is that

of a semi-passive suspension, using alternating fields.

The equation of motion of a charged particle in an alternating electric field is a variant of Matthieu's equation. Given some damping, quasi-stable solutions are possible, in which the particle executes a small oscillation about a stable mean position.

### 2.2.4 Cryomagnetic Suspension

A superconductor is perfectly diamagnetic (the Meissner effect): it is repelled by a magnetic field. It is therefore possible for a small permanent magnet to be stably suspended over a superconducting surface, without requiring any ancillary stabilization equipment. This phenomenon provides the basis for a simple and effective suspension system.

Despite the difficulty of operation at cryogenic temperatures, it was considered that this type of suspension offered the simplest mechanization and also the best compatibility with the other LLAMA components of all the possible field supports. Later chapters of this report describe the development of this concept into an operational system.

## 2.3 Displacement Detection

Starting from rest at $10^{-6}$g, 0.45 seconds are required to move through a distance of one micron. For a given acceleration, the bandwidth of an accelerometer depends strongly on the sensitivity of the

displacement detection system. In order to maintain an adequate bandwidth, an accuracy of 0.1 micron was set as the design goal for the displacement detector in LLAMA.

An additional reason for limiting the test-mass displacement to very small values is that this minimises the effects of spatial non-linearity of any axial forces. It would otherwise be necessary to obtain a calibration curve for the instrument over the whole range of displacements.

The precision required of the displacement detector is such that interferometric methods offer the most practical solution. A specialized Twyman Green laser interferometer has been designed for LLAMA, in which, by means of a folded optical system, interference is obtained between light beams reflected from small, optically flat and parallel mirrors attached to either end of the test-mass. This technique gives twice the displacement sensitivity of a conventional interferometer and also allows the design of a system which is insensitive to the inevitable small oscillations of the test-mass about transverse axes.

## 2.4 Restoring Force Generation

At the acceleration levels for which LLAMA is designed, the maximum restoring force required is of the order of one microgram, for a test-mass of about one gram. Methods of generating, controlling and measuring such very small forces are described in the Master's thesis by Mr S. Ezekiel[8]. Since the test-mass is a permanent

magnet, the easiest technique is to control its position by means of currents in suitably placed small coils, and this approach has been adopted in the initial LLAMA system.

## 2.5 Calibration

As noted in Section 1.2, a primary consideration in the design of LLAMA was that it should not require an externally applied acceleration for calibration. The alternative is, of course, to apply a known small force directly to the test-mass. The most convenient source of such a force is radiation pressure from a mercury arc lamp[8]. The maximum power needed in the calibration beam is of the order of one watt.

## 2.6 Damping

In the LLAMA suspension as finally developed (see Section 4.2) an adequate damping of transverse motion of the test-mass is provided by eddy-current generation in a surrounding copper jacket. The same mechanism gives some axial damping, which may be increased by suitable filtering in the restoring force generation servo (see below).

## 2.7 System Aspects

Figure 3 shows the manner in which the components described above are combined in the complete LLAMA system. The test-mass is a small permanent magnet, which is freely suspended inside a

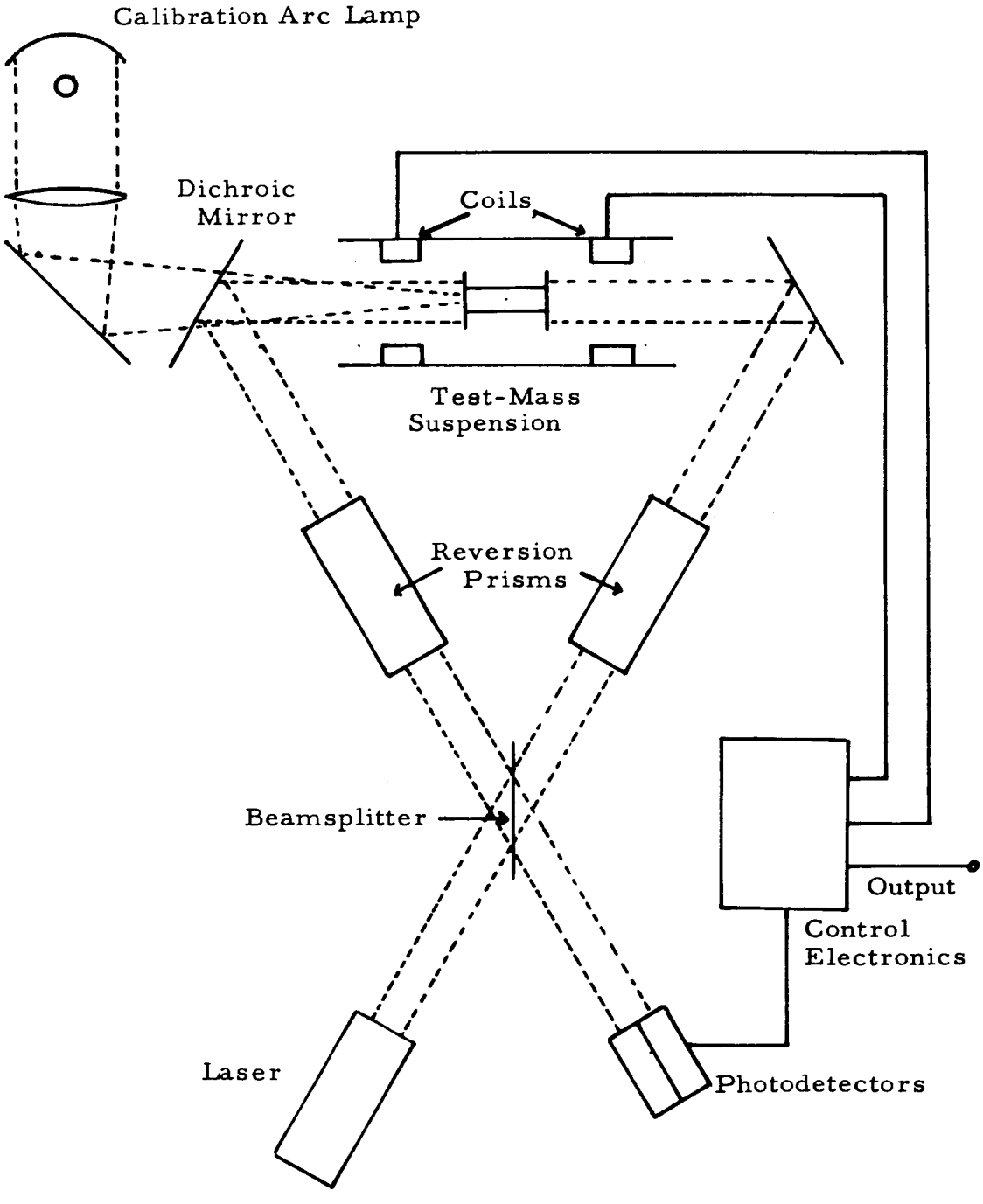


Figure 3: The LLAMA System

superconducting tube. Small optically flat mirrors are attached to the ends of the magnet, to form the fundamental mirrors in an interferometric displacement detection system. The interferometer produces an output signal whenever the test-mass is displaced from the null position in the center of the tube, and this signal is used to control the differential current in two small coils inside the superconducting tube, so as to provide a restoring force which keeps the test-mass very close to the null position. The output of the accelerometer consists of a measurement of the differential current in the coils, in the steady state.

Provision is made to calibrate the instrument periodically by allowing the beam of light from a mercury arc lamp to fall directly on the test-mass and noting the resultant output. The calibration and displacement detection beams are distinguished by color separation. The interferometer uses a helium-neon CW laser at 6328 Å: the mercury arc has a low output at this wavelength, which is further reduced by a rejection interference filter centered on the laser wavelength.

# CHAPTER III

# THE MEISSNER EFFECT SUSPENSION

## 3.1 Superconductivity

The phenomenon of superconductivity was discovered by H. Kamerlingh-Onnes at the University of Leiden in 1911[9], when he observed that the electrical resistance of mercury disappeared at a temperature of 4.15°K. While of course it cannot be stated categorically that a superconductor exhibits truly zero resistivity, an upper limit of $10^{-23}$ ohm. cm has been established[10].

A total of 24 elements and a great number of alloys and compounds[11] are now known to exhibit superconductivity. For bulk samples of pure metals, the change from the normal to the zero-resistance state is abrupt as the temperature is reduced (see Fig. 4), at least in the absence of a magnetic field, and the transition temperature is characteristic of the material, ranging from 0.35°K for hafnium (although lower transition temperatures will undoubtedly be found as cryogenic technology allows lower temperatures to be explored) to about 18°K for certain alloys of niobium and zirconium.

The transition temperature of a given sample is strongly affected by the magnitude and direction of any applied magnetic field. For a given specimen shape and orientation with respect to the field

the critical field (defined as that field above which the material is in the normal state) has an approximately parabolic dependence on the temperature:

$$H_e \cong H_o \left( 1 - \left( \frac{T}{T_c} \right)^2 \right) \qquad \ldots (3.1)$$

where $T_c$ is the transition temperature at zero field and $H_o$ is the critical field at zero temperature.

Because superconductors are perfectly diamagnetic (see below), when a given specimen is inserted into a constant field the actual field intensity at the surface will vary in a way which is dependent on the specimen shape and its orientation with respect to the field. The actual critical field is then given by

$$H_e = (1-n) H_c \qquad \ldots (3.2)$$

where $H_c$, the maximum possible critical field for a given temperature and material, is obtained when the specimen is a long cylinder oriented parallel to the applied field (i.e., n=0 for this case). For a cylinder perpendicular to the field, n=1/2; for a sphere, n= 1/3; this parameter is known as the demagnetizing coefficient for the specimen.

When the field is between $H_e$ and $H_c$, the specimen is in a complex state wherein some regions are superconducting and some are normal[12].

For the purpose of suspending a magnet over a superconducting

surface, these complexities may fortunately be ignored. It is sufficient to state that the field due to the magnet at the surface of the superconductor must not exceed $H_c$, which is of course related to the temperature by an equation similar to (3.1), with $H_o$ replaced by $H'_o$, the critical field at zero temperature and demagnetizing coefficient.

Figure 5 shows $H_c$ versus temperature for several materials.

Apart from the above magnetic effects, until 1933 it was assumed that the magnetic properties of a superconductor were those of a perfect conductor. In that year Meissner and Ochsenfeld found that all magnetic flux is expelled from the interior of a superconductor as it makes the transition from the normal state[13]. The Meissner effect was a radical discovery, which could not be predicted on the basis of any previous experiments. The implication for the present purpose is that any external magnetic field has a zero normal component at the surface of a superconductor, so that it behaves like a perfect diamagnet.

There have been many attempts at theoretical explanations of superconductive phenomena. One result from the Londons' theory[14] which is of interest in the present context is that the magnetic field inside a superconductor is not identically zero, but decreases from the surface according to

$$\nabla^2 \underline{H} = \underline{H}/\lambda^2 \qquad \ldots (3.3)$$

If supercurrents are flowing, the current density obeys a similar law:

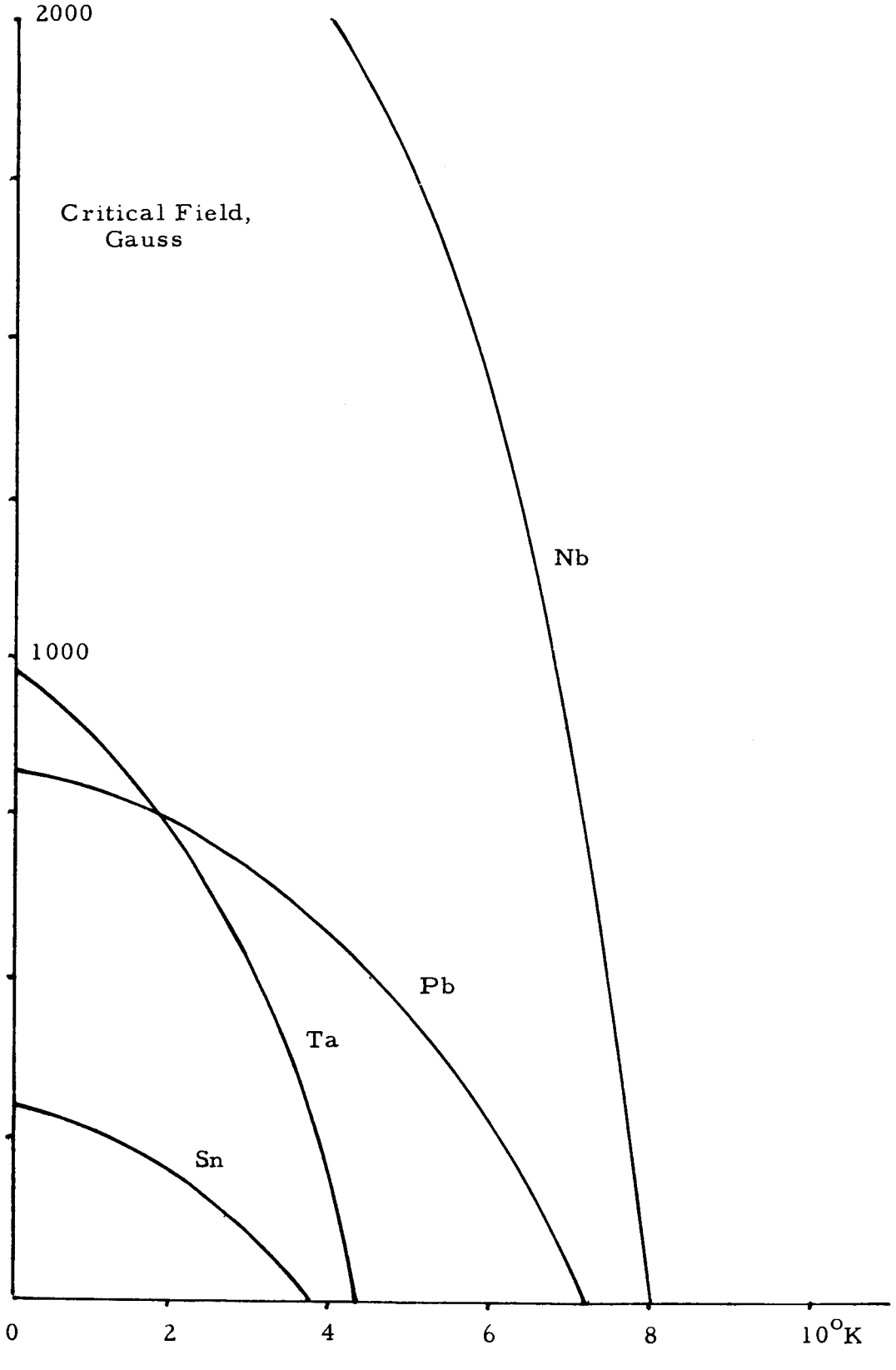


Figure 5: Critical Field of Several Superconductors

$$\nabla^2 \underline{J} = \underline{J}/\lambda^2 \qquad \ldots (3.4)$$

For bulk specimens, these equations lead to an exponential decrease of magnetic field and current density with distance from the surface. The penetration depth $\lambda$ is of the order of $10^{-5}$ to $10^{-6}$ cm, depending on the material.

As noted in Section 5. 5, it is proposed to use a thin film of superconductive material in a later version of the LLAMA suspension. The significance of the above result is that the film must be at least several microns thick.

The Londons' theory, in common with most other more-or-less successful descriptions of superconductive phenomena, was phenomenological in that it made rather arbitrary assumptions in order to explain experimental results. It is only quite recently that a theory has been proposed which holds promise of explaining the observed effects in any detailed and self-consistent way. This new theory, known as the BCS theory (being developed by Bardeen, Cooper and Schrieffer at the University of Illinois in 1957)[15], makes a basic advance in that it recognizes the importance of electron-phonon interactions. In a pure conductor, the major interactions of the conduction electrons consist of Coulomb repulsion and a weak two-particle attraction by phonon interchange (i. e., energy exchange via crystal lattice vibrations). It can be shown that the phonon interaction at low temperatures in an ideal metal leads to a 'pairing' of the electrons so that the net momentum of each pair is the same. Since

this effect is stable with respect to small disturbances (for instance, local scattering by lattice imperfections), the electrons no longer obey the normal statistical rules: once each pair has been given a net momentum by some external force, this momentum persists, representing a stable circulating current.

## 3.2 The Floating Magnet

Consider a small permanent magnet placed over a large, horizontal superconducting plane. As was first demonstrated by Arkadiev[16], the diamagnetism of the superconductor may produce a repulsion which is sufficient to overcome the weight of the magnet, causing it to be stably suspended.

A more pictorial way of thinking of this phenomenon is the following: At this macroscopic level, the small penetration of the field into the superconductor may be neglected. The lines of force near the superconductor must therefore be parallel to the surface. The resulting field distribution is identical to that which would be produced (without the superconductor) by the magnet together with an 'image' of the same sign an equal distance below the surface. The height at which the magnet will float over the superconductor is therefore equal to half the height at which it could just be supported by an identical magnet.

When the magnet moves over the superconducting surface, the image moves with it. The system is therefore neutrally stable with respect to horizontal displacement, and constitutes an essentially

'stictionless' suspension.

Once a means of establishing a suitable superconducting surface has been provided, the Meissner effect suspension is extremely simple, as compared with the systems discussed in Sections 2.2.1 to 2.2.3, because it does not require feedback techniques to ensure vertical stability. In addition, quite substantial float heights (at least 1 cm) may be obtained, minimising forces due to surface roughness, etc.

### 3.2.1 The Cryogenic Gyro

A considerable amount of effort has been devoted during the last decade to the application of the Meissner effect as a frictionless bearing for gyros and small instrument motors. In general, the approach has been the converse of that suggested for LLAMA, in that a superconducting body has been levitated in a magnetic field.

The advantage of this technique, of course, is that one is not limited by the flux densities available from a permanent magnet, so that fairly heavy bodies may be floated. For example, Harding and Tuffins [17] have experimented with a niobium sphere weighing 300 gm: as the low friction support allows such rotors to be spun at speeds in excess of 20,000 rpm, the potentialities for gyroscopic applications are obvious.

For stable support of a spherical rotor, a mechanical potential minimum must be exhibited, which is quite simple to arrange with a suitable array of coils. For the LLAMA application, however,

it is almost as difficult to obtain a sufficiently homogeneous field using this technique as in the magnetic suspension discussed in Section 2. 2. 1.

An even more serious difficulty arises because the suspended body is very effectively thermally isolated from its surroundings, including the cooling system, so that any radiant heat influx may cause it to go normal. In fact, Simon[18] found that too low a gas pressure in a superconducting bearing of this type caused his suspended ball to go normal, due to a lack of convective dissipation of the small heat influx through an observation port. In general, a compromise must be found between low gas drag on the one hand and adequate cooling of the rotor on the other.

In the LLAMA system, it is proposed to use radiation pressure for calibration, with a consequent power influx to the test-mass of up to one watt. It is extremely doubtful whether it is possible to obtain sufficiently high reflectivity of the end mirrors and sufficiently good radiative and/or convective cooling to maintain a superconductive test-mass.

However, in view of the magnet simulation possibilities mentioned in the next section, this question of test-mass cooling will be investigated experimentally when the entire system is operative.

## 3.3 Choice of Magnet

The most powerful permanent magnetic material readily available in the form of small bars is Alnico V, which has an attainable BH product of 0.21 ergs/cc. Cylindrical magnets of diameter 0.318 cm (1/8") were chosen. From the manufacturer's published data, magnets with a permeance coefficient of 20, corresponding to a length to diameter ratio of 5, exhibit the maximum value of BH product.

The data presented by the manufacturer allow the calculation of the flux density at the center of a given bar magnet. However, the pole strength, and hence the expected float height, is not derivable directly from these data. In addition, one cannot be certain that the magnets being used are actually magnetised to saturation.

In order to evaluate realistically the height at which the magnet could be expected to float, as a function of its length, bars cut to various lengths in pairs were obtained. These were freshly magnetised, and the jig shown in Figure 6 was used to determine the height at which each magnet would just support its mate. In these experiments, the upper magnet was raised very slowly until the lower one dropped, the separation at this time being twice the float height of the bar under test. The results are plotted in Figure 7.

It is apparent that the float height does not depend very critically on magnet length. In order to minimise the power required in the calibration light beam, the test mass should be as light as possible, so bars of length 1.6 cm and mass 0.9 gm were chosen.

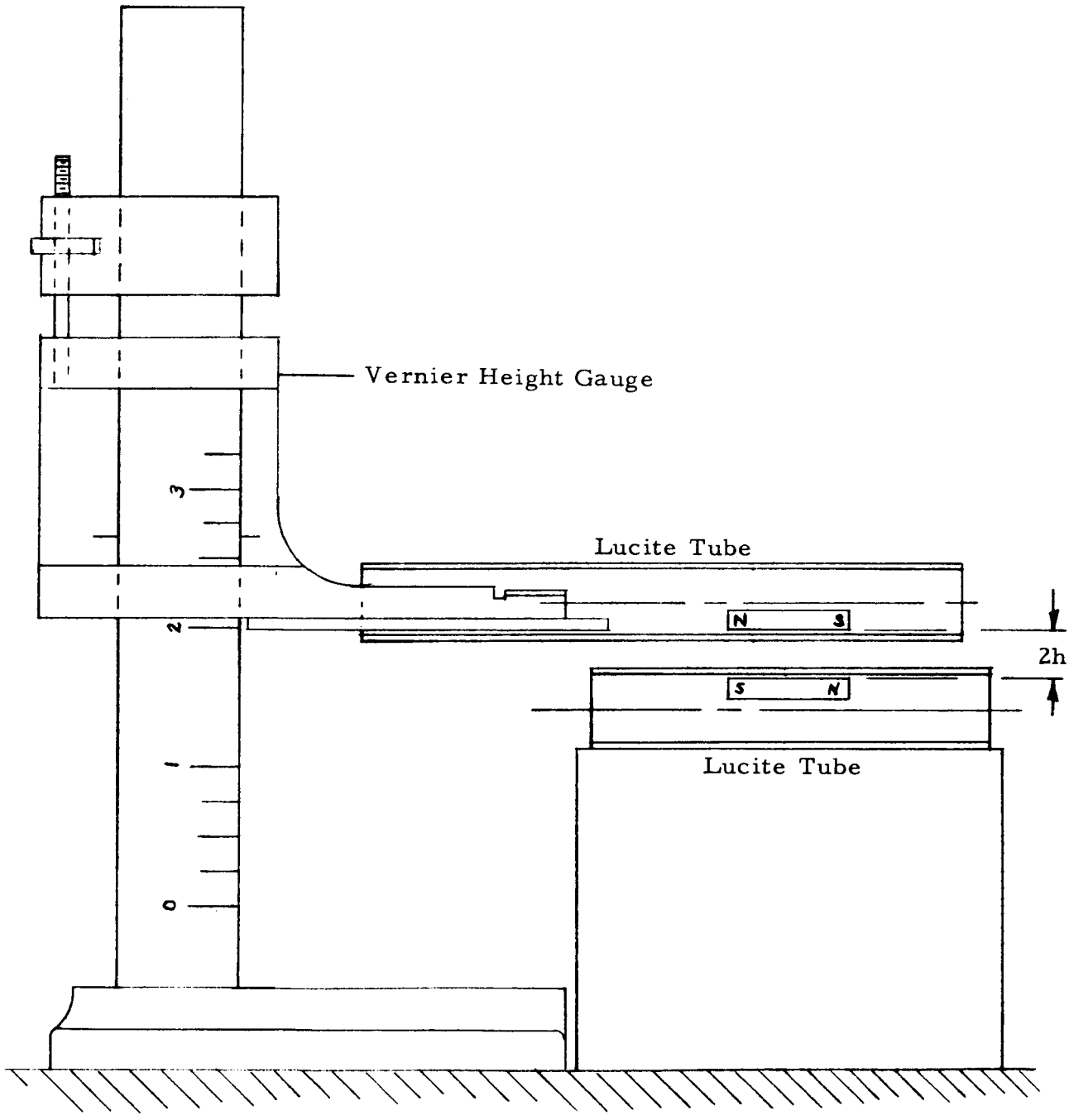


Figure 6: The Float-Height Test Jig

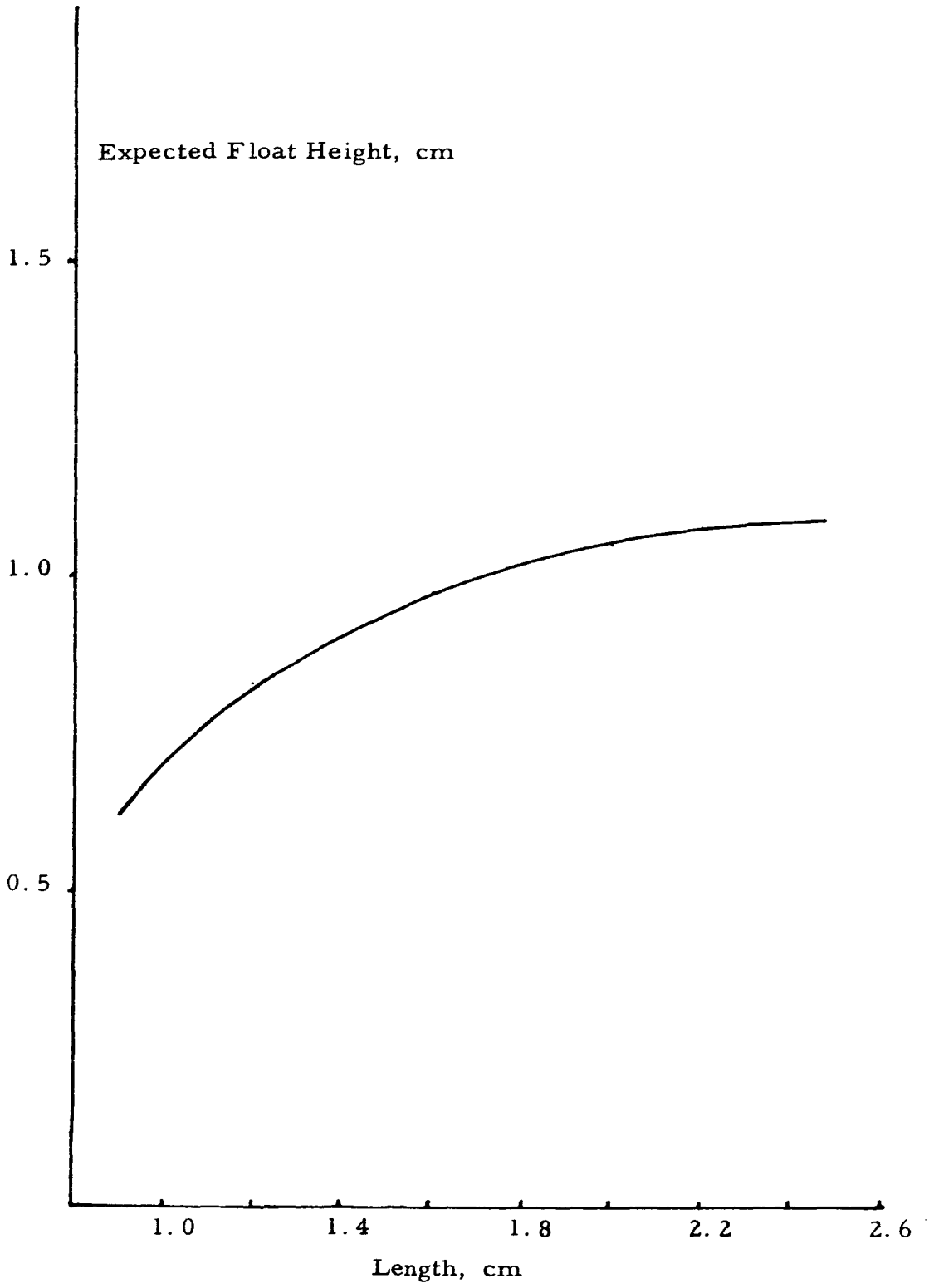


Figure 7: Float Height vs. Magnet Length

As a rough check on this choice, a shallow lead dish was placed in a transparent dewar, as sketched in Figure 8. The inner vessel was filled with liquid helium, and the chosen magnet was lowered into the dish by means of non-magnetic tongs. It was observed that the magnet floated at a height of about 1 cm over the lead surface. Boiling of the helium caused the little bar to dash about at random in the dish.

Although the float heights obtainable with this Alnico V magnet are quite adequate for the present purpose, it is interesting to consider the possibility of suspending the test-mass at a greater height by simulating a permanent magnet with a shorted superconducting coil. The maximum flux density from a permanent magnet is of the order of 10,000 gauss, whereas a small multiturn coil of niobium-zircomium wire, with the maximum persistent current flowing in it, might give a flux density almost an order of magnitude higher. Considerably higher pole-strength to mass ratios might thus be observed. In addition, the problem of starting such a persistent current after the suspension is superconducting would probably be simpler than that of inserting the test-mass after the dewar is filled (see Section 4.2).

However, the test-mass cooling problem discussed in Section 3.2.1 would make this system difficult to implement with the present configuration of LLAMA.

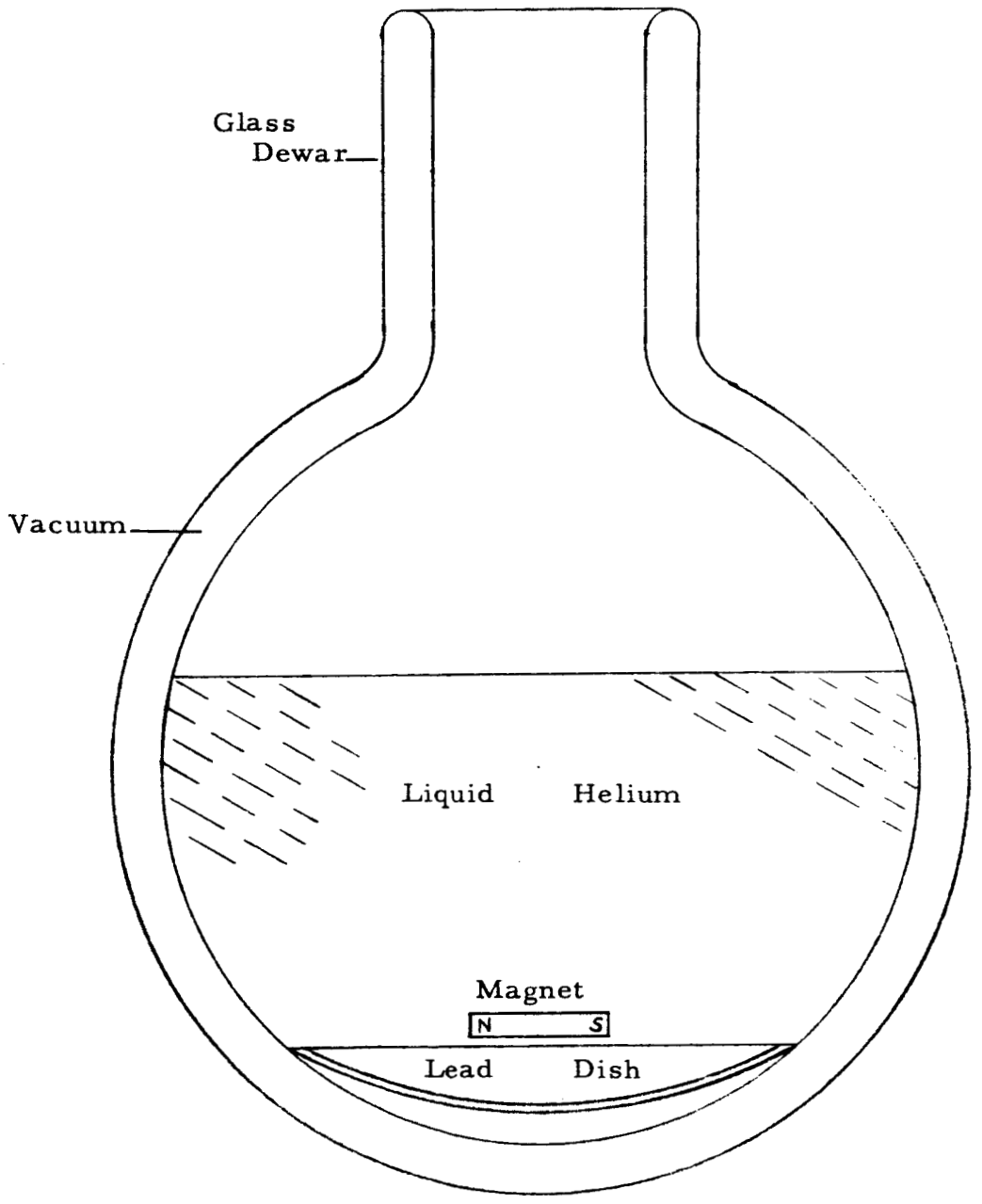


Figure 8: The First Flotation Experiment

## 3.4 Suspension Geometry

The superconducting plane discussed so far allows the magnet to move freely in two dimensions. In order to make a single-axis device, a superconducting trough may be used. The magnet then encounters a restoring force on displacement in any direction except along the axis of the trough.

Unfortunately, the image concept used in discussing the superconducting plane is not applicable to this case. Qualitatively, however, one might expect that the float height would be greater in the case of a trough of semicircular cross-section than in the case of the plane.

For discussing qualitatively the behavior of the floating magnet, another simple mental picture may be used to replace the image concept. Since the energy stored locally in the magnetic field is proportional to the square of the field strength, the magnet tends to move in such a way that the lines of force are separated as widely as possible, this being the minimum-energy configuration. The magnet therefore behaves as though there were a repulsion between the lines of force in its field.

In particular, this concept allows a discussion of edge effects. When the magnet is near an edge of the superconducting surface, some of the field 'spills over', forcing some of the lines of force to double back on themselves, as sketched in Figure 9. The repulsion between the lines then has a component parallel to the surface of the superconductor,

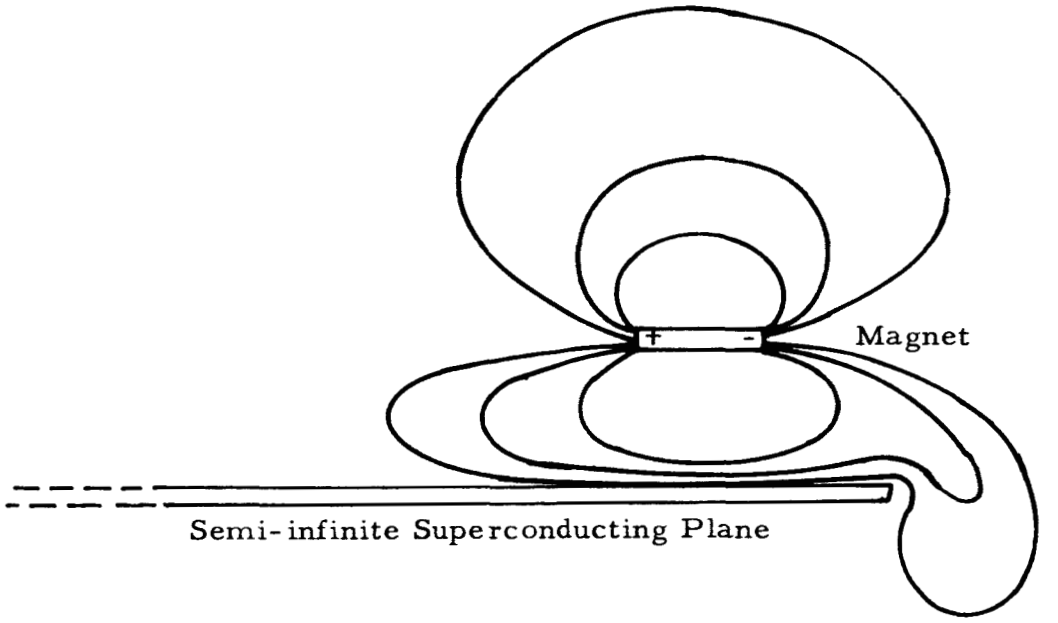


Note: This figure is not intended to be an accurate representation of the field, but simply to give a qualitative impression of why a floating magnet is drawn to the edge of a superconducting surface.

Figure 9: Field Distortion at Edge of Superconducting Plane

and the magnet is attracted to the edge. A finite plane therefore gives a suspension which is unstable in the horizontal direction.

In a semicircular trough of small radius, the magnet may float near or even above the axis. Because of the edge effect, the suspension is then unstable with respect to transverse horizontal displacement, and the magnet will be ejected. The obvious solution to this problem is to use a superconducting tube rather than a trough.

A tubular geometry has two incidental advantages as compared with a trough: (a) the suspension is 'tighter' with respect to transverse displacements, so that transverse oscillations have a higher frequency and hence may be damped more readily, and (b) since the magnet is almost completely surrounded by superconductor, of permeability zero (which is of course what is meant by perfect diamagnetism), it is well shielded from external fields.

Topologically speaking, a tube is a doubly-connected structure, which means that any motion of the magnet will set up persistent currents, so that the support itself will develop a magnetic moment. A singly-connected tube may be constructed by introducing a barrier consisting of a narrow slit along the upper surface of the tube*. A small amount of flux from the magnet will then leak out through the slit, and variations in the width of the slit will produce axial forces, which cannot be tolerated. The slit must therefore be made with great care.

*A possible use of a multiply-connected suspension is discussed in Section 5. 5.

The magnet will of course always float at a lower height in a tube than in a trough of the same radius of curvature. Indeed, for a tube with a slit of negligible width, the magnet will always float below the axis, regardless of the radius, since it would, by symmetry, float on the axis in the absence of gravity.

A slitless tube creates sufficiently simple boundary conditions for analytical treatment (see Appendix), but the introduction of a slit complicates the field distribution considerably. Because of the compression of the field inside the tube, there is a strong tendency for flux to be 'squeezed' out through even a narrow slit. This produces a levitating force on the magnet, so that, as far as float height is concerned, there exists an optimum slit width.

Because of the end effects, a tubular suspension is normally axially unstable, and some means must be found of compensating the inherent axial forces. The introduction of a slit greatly complicates the situation, but, for the purposes of discussion, it will be assumed that the end effects produce axial forces which vary with the displacement in the manner prescribed by Eq. (A. 33) of the Appendix:

$$F = \alpha \sinh 2c_1 x \qquad \ldots (3.5)$$

where x is the displacement, $c_1$ is a constant equal to 3.83 divided by the radius of the tube, and $\alpha$ is to be regarded as an experimentally determined constant.

## 3.5 End-Effect Compensation

Several different end-effect compensation techniques were conceived during the development of LLAMA. Because of their simplicity and flexibility, stabilization is achieved by means of small coils inside the suspension in the first model of the instrument. These coils also serve as the source of restoring force in closed-loop operation[8].

Other promising compensation methods are discussed in Section 5.5, as subjects for future investigation.

A permanent magnet may be attracted or repelled by a current-carrying coil, depending on the sense of the current relative to the orientation of the magnet. If coils are placed on either side of the center of the suspension, with their axes coincident with the axis of the tube, and fed with an appropriate current, it is possible to overcome the forces due to the suspension and produce a mechanical potential minimum. This implies that the magnet is repelled by the coils, which normally would give rise to a rotationally unstable situation: however, reaction from the sides of the tube prevents this problem from arising in normal operation. This effect does limit the current which can be used to fairly small values, but effective end-effect compensation is quite possible.

According to Eq. (A.37) of the Appendix, the force produced by a pair of stabilizing coils is of the form

$$F_c = -\beta I \sinh c_1 x \qquad \ldots (3.6)$$

It is only possible to produce exact compensation for displacements which are so small that both (3.5) and (3.6) are effectively linear. For a tube of radius 1.25 cm, this condition holds within 0.02 % up to a displacement of 60 microns, and within 1% to 400 microns. If the displacement can be held within one micron, as is expected when the entire LLAMA system is operational, the maximum uncompensated end effect force would, according to this model, be no more than $3.10^{-11}\alpha$ dynes. This is so small that in practice essentially perfect compensation may be achieved.

The non-linearity of these equations does however have some important consequences in the test of the suspension (Section 5.2).

## 3.6 The Flux-Trap Problem

In the discussion so far, it has been tacitly assumed that the superconducting surface was continuous. This is only true if certain precautions are taken during the cooling process.

Suppose that a sheet of superconducting material, in the normal state, is immersed in a magnetic field, which for simplicity is taken to be normal to the surface. If there exists a local maximum of field intensity, the region near the maximum will remain normal after the rest of the sheet is superconducting, as the sheet is cooled uniformly, because of the dependence of transition temperature on

the applied field (Section 3.1). There will thus be a 'hole' in the superconductor with flux passing through it. As the magnetic field cannot penetrate the superconductor, there is no way for this flux to escape. As the sheet is cooled further, the size of the hole will decrease, but the same amount of flux will pass through it: the field intensity in the hole will increase until it reaches the critical field corresponding to the temperature of the sheet.

If now the source of the field be removed, a current will be induced around the hole. Since there is no resistance, Faraday's law gives (in m.k.s. units)

$$V = L\frac{dI}{dt} = -\frac{d\Phi}{dt} \qquad \ldots (3.7)$$

where L is the self-inductance of the circuit around the hole and $\Phi$ is the flux due to the external source.

Thus, by the definition of self-inductance, the flux in the hole due to the induced current is

$$\Phi' = LI = \Phi_o - \Phi \qquad \ldots (3.8)$$

which is just sufficient to maintain the total flux at the value it had before the source was removed: $\Phi_o$.

Once flux has been trapped by a superconductor, there is thus no way to eliminate it short of raising the temperature above the zero-field transition value and recooling.

The conclusion, then, is that there must be no closed contours of magnetic field intensity surrounding maxima on the surface of the superconductor at the time that it is cooled. If it is desired to have the test-mass magnet in the vicinity of the suspension during the cooling process, it must be located so that the nearest part of the superconductor is an edge of the surface.

A similar problem arises if the cooling is not uniform. If a sheet of superconductor be immersed in a uniform field and cooled from the edges, the peripheral region will superconduct first, trapping the flux passing through the center of the sheet. Thus the cooling technique must be such that no local maximum of temperature occurs at any time.

The influence of these phenomena on the design of the LLAMA suspension is discussed in Section 4. 2.

## 3.7 Ultimate Limits of Performance

The most significant feature of the LLAMA suspension is that there is no mechanism present which might cause 'stiction'. The threshold sensitivity which might conceivably be attained is therefore limited by other factors, such as the sensitivity of the displacement detector and the geometric perfection of the superconducting surface.

One possible limiting factor is thermal fluctuation of the test-mass position (i. e., Brownian motion of the test-mass). If the threshold sensitivity of the displacement detector is $x_o$ cm, and it

is required to detect an acceleration of $a_o$ cm / sec$^2$, then it is clear that the maximum spring constant of the accelerometer (whether it be generated by feedback or by open-loop forces) is given by

$$K = \frac{ma_o}{x_o} \qquad \ldots (3.9)$$

The mean amplitude $x_n$ of Brownian oscillation of the test-mass is then given by the equipartition theorem as

$$\frac{ma_o x_n^2}{2x_o} = \frac{kT}{2} \qquad \ldots (3.10)$$

where k is Boltzmann's constant, $1.38 \times 10^{-16}$ ergs/degree, and T is the absolute temperature.

Assuming that measurement is possible when the amplitude of the Brownian oscillation is one half the displacement threshold, the acceleration threshold is given by

$$a_o = \frac{4kT}{mx_o} \qquad \ldots (3.11)$$

The implication of this equation is that this limit is minimised by allowing a large $x_o$; but unfortunately the natural period $\tau$, and hence the settling time of the instrument, is proportional to $\sqrt{x_o}$. The limitation is therefore likely to be the patience of the observer (or perhaps the supply of helium!). Putting $x_o$ = 1 micron and T=10$^o$ in (3.11) gives

$$a_o = 5 \times 10^{-12} \text{ cm/sec}^2 \qquad \ldots (3.12a)$$

$$\tau = 8 \text{ hours} \qquad \ldots (3.12b)$$

From (3.9),

$$\tau = 2\pi \sqrt{\left(\frac{x_o}{a_o}\right)} \qquad \ldots (3.13)$$

so that (3.11) may be written

$$a_o = \frac{2\pi}{\tau} \sqrt{\left(\frac{4kT}{m}\right)} \qquad \ldots (3.14)$$

Thus the acceleration threshold imposed by thermal fluctuation varies inversely as the allowable natural period. Increasing $x_o$ to 1 mm would improve the value of $a_o$ given in (3.12a) by a factor of one thousand, but it would also increase the natural period to about one year. For most cases, then, $10^{-12}$ cm/sec$^2$ may be taken as a practical limit on the sensitivity.

Another possible limit is imposed by thermal fluctuation of the current in the restoring coils, which is given by

$$\Delta I = \sqrt{\left(\frac{4kTB}{R}\right)} \qquad \ldots (3.15)$$

where R is the output resistance of the current supply, and T is now room temperature. Because of (3.14), there is no point in having a large value of the bandwidth B.

For small displacements, the corresponding change in the spring constant is given by (3.6) as

$$\Delta K = c_1 \beta \, \Delta I \qquad \ldots (3.16)$$

In the experimental suspension, $c_1 \beta = 1.5$ dynes/cm/mA (see Section 5.3). Taking as an example B= 0.001 c/s, R= 10kΩ,

Eqs. (3.15) and (3.16) give for this case

$$\Delta K = 2.10^{-7} \text{ dynes/cm} \qquad \ldots (3.17)$$

For comparison, the spring constant in the Brownian motion limited case of (3.12) is given by (3.9) as

$$K = 5.10^{-8} \text{ dynes/cm} \qquad \ldots (3.18)$$

It should not be difficult to decrease $\Delta K$ by two orders of magnitude, by increasing R and decreasing $\beta$ (according to (A.37) of the Appendix, $\beta$ decreases exponentially with separation of the coils). The conclusion is therefore that thermal fluctuation of the spring constant imposes a sensitivity limit which is of the same order as that imposed by the Brownian motion effect.

The limitation imposed by distortion of the superconductor is not expected to be significant at the above levels. Large scale distortion (buckling) simply modifies the inherent spring constant of the suspension, at least for small displacements, and hence may be compensated by adjusting the current in the stabilizing coils. Surface roughness is averaged over a distance of the order of the float height, so that, again for small displacements, it too is seen simply as a variation of the spring constant. If the surface finish is held to (say) 5 microinches, these effects should be negligible.

Finally, the experimental suspension is grossly overdamped for operation at the levels considered in this section (Sec. 4.3). This is due to eddy current generation in a copper liner inside the

superconducting tube. In the ideal case of a magnet floating inside a superconducting tube, with no other metal present, the only damping would be due to eddy current generation in the metal of the magnet itself, since eddy currents in a superconductor can dissipate no energy. The resistivity of Alnico V is 2500 times that of copper, so that it is expected that a suspension of this type would not be limited by damping at the levels considered.

In view of the above results, it is clear that the ultimate limit on sensitivity, at least in a terrestrial installation, will be due to external vibration, microseisms, etc. It is only in a space application that LLAMA will ever be able to approach its maximum performance potential.

In this discussion of limits on performance, it has been assumed that the only variation of the currents in the coils is due to thermal noise. If end effect compensation requires a current which is large compared to the position control (restoring force) currents, it may be impossible to regulate the current sufficiently for this to be so. This is not regarded as a fundamental limitation, however, since it is possible to reduce the required stabilizing currents to an arbitrarily low level, by increasing the length of the suspension or by one of the end effect compensation schemes discussed in Section 5. 5.

# CHAPTER IV

# PRACTICAL SUSPENSION DESIGN

## 4.1 Preliminary Experiments

In order to gain some familiarity with the problems of cryogenic suspension operation, a series of experiments were performed in the transparent glass dewar sketched in Figure 8. Because this dewar was unsilvered, there was a large radiant influx of heat from the surroundings, with the result that the liquid helium boiled away quite rapidly, limiting the duration of each experiment to about ten minutes. The boiling helium produced rather turbulent conditions inside the dewar, so that it was difficult to make estimates of the forces on the floating magnet. In addition, the rapid efflux of cold helium from the top of the dewar caused a heavy fog, which at times prevented photography or even observation of the interior.

For these reasons, the experiments were generally rather qualitative; however, a great deal of experience and some quite significant information was obtained.

The first experiment consisted simply of a demonstration that a small magnet would indeed float over a lead dish, as described in Section 3.3.

For the next experiment, a lead tube was constructed, as

shown in Figure 10. The upper edges were separated by a sliver of cardboard, so as to make the superconductor singly connected. In order to keep the magnet in the tube, the ends were closed with a grid of (non-superconducting) wires. The magnet was prepared by attaching to the ends lucite discs, about a centimeter in diameter, to simulate the mirrors which would be present in the actual device.

The magnet was then inserted into the cylinder, and the whole assembly lowered on strings into the dewar full of liquid helium. As the lead cooled, the magnet did not lift itself off, but it was possible to get it floating by flicking it with a bent probe lowered into the dewar. However, the float height was very disappointing: the lucite discs barely cleared the surface. It was found that by shaking the tube, it was possible to start the magnet spinning about its long axis, which showed that it was freely suspended.

The reason for the poor float height in this experiment was, of course, the flux-trapping problem discussed in Section 3.6. This hypothesis was confirmed by a later experiment (see below).

A new tube was now constructed, as shown in Figure 11. A lucite tube of suitable diameter was cut in half lengthwise, and a wide slot was cut in the top, near the center. Lucite discs were glued to the inside of this semi-cylinder, the purpose being to keep the magnet in the low-force region near the center of the suspension. The device was completed by attaching to the outside a sheet of niobium formed into a section of a cylinder, with a gap about $60^{\circ}$ wide at the top.

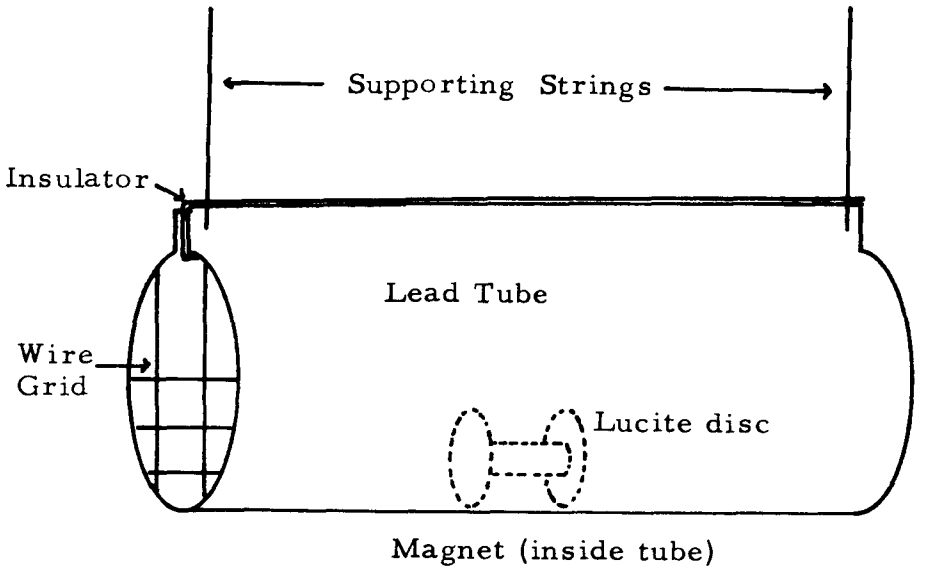


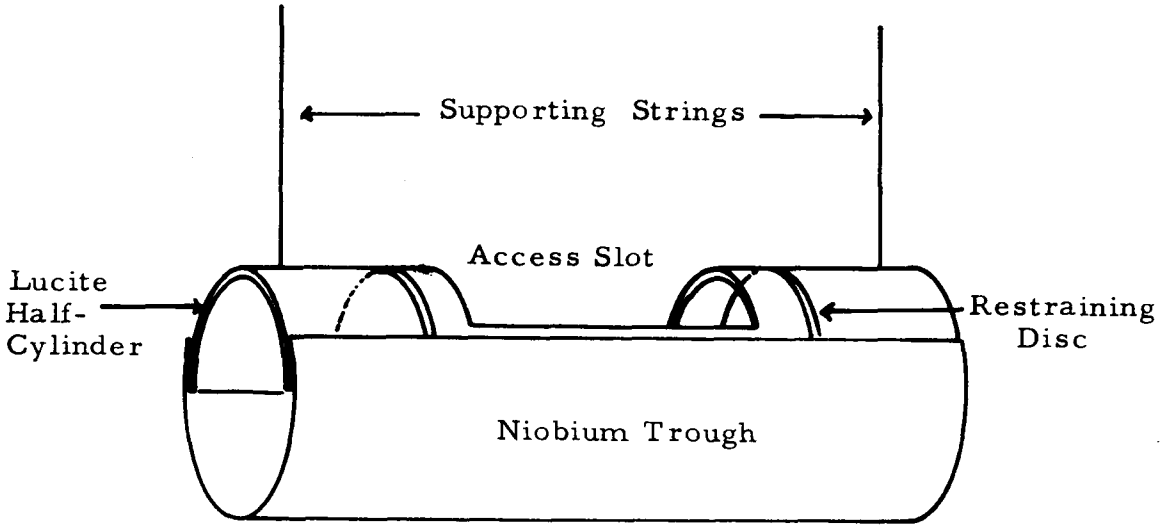


Figures 10 and 11: Early Experimental Suspensions

This assembly was suspended on strings inside the dewar of helium. When it was certain that the niobium was superconducting, the magnet was lowered with non-magnetic tongs and inserted into the support through the slot in the lucite.

The magnet floated just below the axis, and moved very easily between the lucite discs when the tube was tilted slightly. While it was not possible to make a quantitative estimate of the axial forces, this experiment did indicate that there were no unexpected gross phenomena which might prevent the operation of the system.

In order to confirm the importance of the flux-trapping effect, this experiment was repeated, with the magnet placed in the tube before it was inserted into the dewar. It was observed that the magnet did not lift off the superconducting surface, and when it was flicked with a probe, it floated with a very small clearance. Movement of the magnet in the axial direction was very sluggish.

## 4.2 The LLAMA Dewar

The overall configuration of LLAMA, together with the lessons learned in the preliminary experiments, dictated the following requirements for a dewar which would permit quantitative performance measurements:

i) The suspension itself should consist of a superconducting cylinder, with an axial slit along the top to prevent circulating supercurrents.
ii) The inside of the cylinder, where the magnet would float, should

be evacuated to at least $10^{-6}$ torr, to prevent radiometer effect from interfering with light-pressure calibration of the instrument[8].

iii) Optically flat windows should be provided at the ends of the cylinder, to allow access of the light used in the calibration and in the interferometric displacement detector.

iv) Some means should be provided for storing the magnet externally to the suspension during the cooling process, to avoid flux-trapping.

v) The ratio of liquid helium capacity to total heat input should be such that operation for at least two hours would be possible, to allow time for careful measurements.

vi) No magnetic materials should be used in the construction of the dewar.

The construction of a dewar meeting these specifications was sub-contracted to Janis Research, Inc., of Stoneham, Mass. The resulting apparatus is shown in the frontispiece and, in cross-section, in Figure 12.

The inner vessel, having a capacity of about two litres, was made of stainless steel except for the bottom, which was a plate of copper 0.25 inches thick. A copper radiation shield was attached to the inner vessel at the neck, where it was cooled by escaping helium gas. The outer vessel was constructed entirely of stainless steel, and was mounted on a solid base plate to provide a definite reference for levelling purposes.

In the first version of the instrument, the suspension consisted

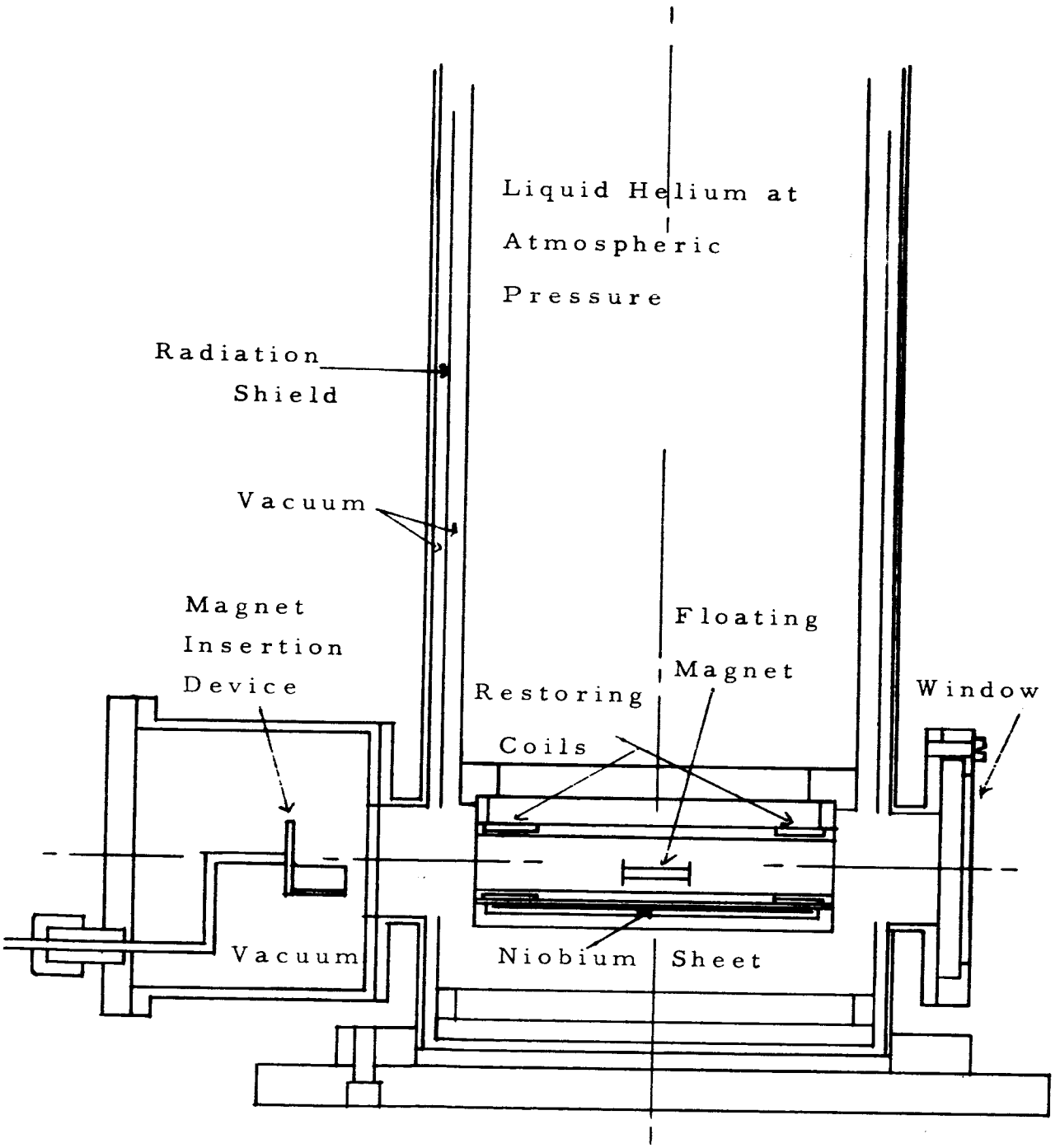


Fig. 12: Cross-Section of the LLAMA Dewar.

of a sheet of niobium attached to the inner surface of a one-inch diameter hole bored lengthwise through a solid copper block, 4.5 inches long. This block was soldered in place over an aperture in the bottom plate of the inner vessel, so that liquid helium was in contact with the top of the block when the dewar was filled. However, the first attempt at operation showed that the thermal resistance between the niobium and the liquid helium was too high: it appeared that the niobium was so close to its zero-field transition temperature ($8^{\circ}K$), at least near the ends of the tube, where the radiant heat input was greatest, that introduction of the magnet exceeded the critical field.

To overcome this problem, the copper block was replaced with a hollow copper box, of the same outside dimensions. Holes were drilled in the ends of the box, and a thin-walled copper tube (outside diameter 2.5 cm) inserted and soldered in place. Niobium sheet was wrapped around the outside of the tube, inside the box, to form a cylinder with an axial slit about $45^{\circ}$ wide at the top*. In operation, liquid helium from the inner vessel of the dewar filled the box, so that the niobium was maintained at $4.2^{\circ}K$, sufficiently low to ensure superconduction in ambient fields of upr to about 2,000 gauss (see Figure 5).

This modification produced an incidental effect of considerable value: as the copper tube was now inside the superconductor, eddy

* The reason for the width of this slit was some concern about the attainable float height, which proved to be groundless. A very much narrower slit will be used in future versions of the instrument (see Section 5.5).

currents were induced whenever the magnet moved. The damping caused thereby proved to be quite substantial: damping ratios of about 0.2 were observed for transverse oscillations of the test-mass. The only motion which was lightly damped was rotation of the magnet about its longitudinal axis, which had a decay time constant of the order of ten minutes. Fortunately, this motion is of no significance in the operation of the instrument.

The copper tube was open at the ends to the dewar vacuum, and holes were provided in the radiation shield and windows in the outer vessel. In practice, the dewar was evacuated to about 0.02 torr before filling with helium; cryopumping (i.e., condensation of residual air on the cold surface of the inner vessel) was relied upon to produce the requisite hard vacuum.

The problem of inserting the magnet into the suspension after cooling of the superconductor was solved, after several quite elaborate schemes had been investigated, by the simple device shown at the left in Figure 12. One of the windows in the outer wall of the dewar was removed, and a cylindrical aluminum antechamber bolted on in its place. The outer end of this cylinder was closed with a lucite window*, using a neoprene gasket as a vacuum seal. The magnet was stored by holding it against the wall of the antechamber with a small external magnet. A lucite spoon was constructed and attached to the

* This was a temporary expedient for preliminary testing of the suspension. An optical flat would of course be required for use with the interferometer.

end of a bent stiff wire passing through a vacuum seal at the bottom of the lucite end-plate, so that it could be manipulated externally.

Insertion of the magnet with this device proved relatively simple. The spoon, when not in use, rested against the wall of the antechamber, and the test-mass was moved over it and allowed to drop. The wire protruding from the feed-through was rotated until the spoon was on the center line of the suspension and then pushed in, carrying the magnet into the superconducting tube. The repulsion from the superconductor tended to rotate the magnet as it approached, so that it was necessary to move through the last few millimeters of travel of the spoon quite rapidly; the momentum thus gained was usually sufficient to propel the magnet deep into the suspension.

The suspension was, of course, axially unstable due to the end effects discussed in Section 3.4. Stabilizing coils (see Section 3.5), each having 1300 turns of #36 copper wire, were placed inside the tube near each end, the leads being brought out through a sealed electrical connector in the outer wall of the dewar. When these coils were fed with a current of about 15mA in series (the sense of course depending on the orientation of the magnet when it was inserted), it was found that the magnet executed a damped axial oscillation, settling near the center of the suspension.

Because of the limited natural damping in the suspension, the velocity with which the magnet was injected from the spoon was rather critical. If it were too small, the repulsion at the end of the

tube due to the superconductor and the nearer coil (for stability inside the suspension, the current in the coil was of course in such a direction that it repelled the magnet) was not overcome, and the magnet flew back into the spoon. On the other hand, if the velocity were too large, the coil at the other end could not stop the magnet, so that it fell out of the tube, where it could not be recovered.

The following technique offered an operational solution to this difficulty: The coil nearest the antechamber was fed with a large current (100 mA) in the attractive sense, the force thus created being considerably larger than the repulsion from the superconductor. When the spoon was inserted into the tube, the magnet lifted off and became stably suspended in the center of the coil. The current was then reduced until the force was just sufficient to stop the magnet being ejected, and the coil at the other end was switched on, in the repulsive sense, with a current of about 15 mA flowing. By means of a center-off reversing switch in the circuit of the nearer coil, the current was periodically interrupted momentarily, producing an axial oscillation of the magnet. By observing the magnet and manipulating the switch in phase with the oscillation, resonance was obtained, the period typically being about one second. At an instant when the magnet was deepest into the suspension, and almost stationary, the switch was flicked all the way over into the reverse position: as the current in both coils was now in the repulsive sense, the magnet was in a stable condition and settled near the center.

Proficiency in this technique required considerable practice,

but it was quite effective. For preliminary testing, however, when the magnet was being inserted and removed rather frequently, it was felt that a simpler method was desirable. The window at the end away from the antechamber was therefore replaced by a lucite disc with a vacuum feed-through in the center. A stiff brass wire, with a lucite disc on the far end, was passed through this seal and inserted into the suspension beyond the coil at that end. The magnet could then be flicked off the spoon into the suspension with a fairly high velocity, since it could no longer fall out the opposite end.

This device proved to be a useful tool, as it enabled the coils to be moved back and forth inside the suspension during testing. It also allowed the magnet to be placed in a definite axial position before the coils were switched on, which was a convenience when experimenting with low currents. However, it could not be used in an operational accelerometer, as it blocked one end window almost completely.

The magnet used in these tests was the same as that in the initial experiments described in Section 4.1 (Alnico V, 0.318 cm diameter, 1.6 cm long) except that it was equipped with aluminum discs at each end, 0.9 cm in diameter, to simulate the mirrors which would be used as part of the displacement detection interferometer. The total weight of the magnet plus ends was 1.1 grams.

The magnet is shown floating inside the suspension in Figure 13. The float height was 1.1 cm, about 1.5 mm below the center line of the superconducting tube. The black annulus around the test-mass in

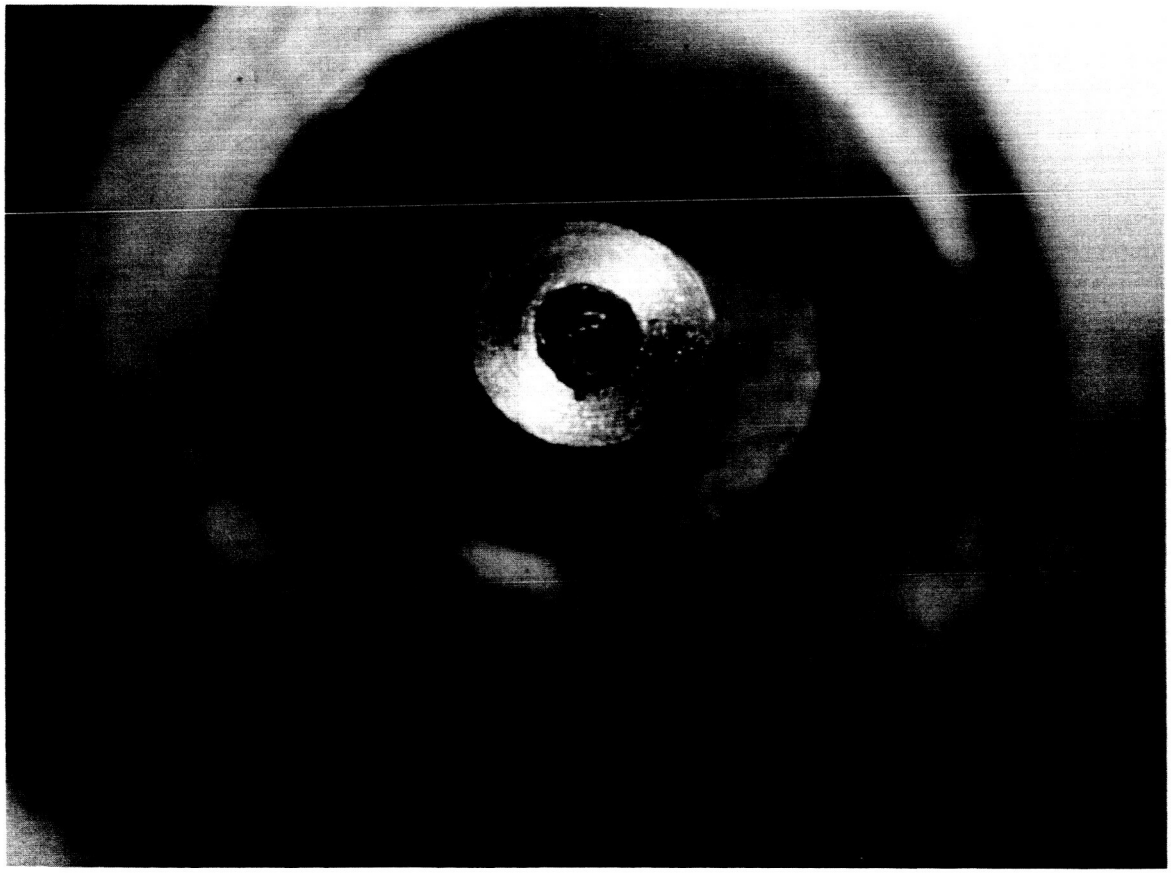

Figure 13: The Magnet Floating in the LLAMA Suspension

the photograph is one of the bobbins for the stabilizing coils, whose inside diameter was 1.7 cm.

It was found that the helium in the dewar was sufficient for operation over a period of 4 to 5 hours. The most significant heat input was probably thermal radiation through the windows in the outer wall of the dewar. The heat conducted along the leads to the coils was calculated as about 70 milliwatts, and the electrical dissipation in the coils was generally of the order of 20 milliwatts. Since the heat of vaporization of liquid helium is 2.7 watt-sec/cc, the presence of the coils resulted in a helium loss of about 2 cc (liquid) per minute. If the copper box containing the suspension were aluminized to reduce radiative losses and if a more efficient thermal design were employed for the coils (e.g., using long, coiled leads to increase the thermal path across the vacuum), the duration of operation could probably be increased by at least an hour.

Use of the calibration arc lamp in the complete LLAMA system will undoubtedly increase the helium boil-off rate, although the output of the lamp is mainly confined to the blue and ultraviolet regions of the spectrum[8]. However, calibration of the instrument is expected to be required, at most, once in every run, so this effect should not be important.

The endurance of the system as presently constituted is considered more than adequate for any contemplated uses. If it should prove necessary, it can of course be prolonged indefinitely by periodic refilling with helium.

CHAPTER V.

# PERFORMANCE OF THE EXPERIMENTAL SUSPENSION

## 5.1 Introduction

The LLAMA suspension dewar, in its present form, demonstrates the feasibility of stably supporting a magnetic test-mass in a superconducting cylinder. However, the technique used for making the tube (see Section 4.2) leaves a great deal to be desired and was adopted only as a simple expedient for checking the design concepts. It is therefore not to be expected that the present suspension should approach the theoretical limits derived in Section 3.7. Modifications to improve the performance are discussed below (Section 5.5).

The best method of testing the suspension would be to observe the performance of the complete LLAMA system. Pending the availability of the other components ( see Section 2.7), an attempt was made to measure the inherent (negative) spring constant of the suspension. There are some problems in making this measurement, which will be clarified by considering the idealized model discussed in the Appendix.

There is serious doubt as to the applicability of the theoretical model to the present suspension; however, conclusions drawn from it do prove to be of some value in interpreting the test data.

## 5.2 The Effect of Axial Non-Linearity

Since measurements could of course be made only when there was sufficient current flowing in the coils to ensure stability, the method used to determine the initial spring constant due to end effects in the suspension consisted of plotting the square of the observed natural frequency of axial oscillation as a function of the current, and extrapolating the resultant curve to zero current. The force on the magnet due to the coils certainly varies linearly with the current, so this method, on the surface, seemed capable of good accuracy, as long as small oscillations were used.

Assuming that the same current is flowing in each coil, and that the coils are equally displaced from the center of the suspension, the maximum tolerable amplitude of oscillation in these tests may be estimated by using Eqs. (3.5) and (3.6). Neglecting damping, the equation of axial motion of the test-mass is

$$m\ddot{x} + \beta I \sinh c_1 x - \alpha \sinh 2c_1 x = 0 \qquad \ldots (5.1)$$

For small oscillations, the motion is of course simple harmonic, with a spring constant given by

$$K_o = c_1(\beta I - 2\alpha) \qquad \ldots (5.2)$$

provided that I is sufficiently large for this quantity to be positive.

For larger oscillations, (5.1) shows that the stiffness of the equivalent spring at first increases with displacement and then starts

to decrease, eventually becoming negative. By differentiating the restoring force in (5. 1) with respect to x, it is easy to show that maxima of the force occur when

$$\cosh^2 c_1 x - \frac{\beta I}{4\alpha} \cosh c_1 x - 1/2 = 0 \qquad \ldots (5.3)$$

The force is zero when

$$\cosh c_1 x = \frac{\beta I}{2\alpha} \qquad \ldots (5.4)$$

and beyond this point is negative, so that this gives an absolute upper limit on the permissible amplitude of oscillation. In practice, it was found that the magnet did not necessarily fly out of the suspension when the displacement exceeded this limit: the restoring force increased rapidly when the magnet approached one of the coils (where the assumptions underlying (A. 37) of the Appendix become invalid, even in the idealized model), so that it was possible for three stable positions of the magnet to exist inside the suspension.

In order to estimate the effect of the amplitude of oscillation on the measured value of the initial negative spring constant $K_s$, consider the average spring constant for an oscillation of amplitude $x_o$, which is given by (5. 1) as

$$\overline{K} = \frac{1}{x_o} (\beta I \sinh c_1 x_o - \alpha \sinh 2c_1 x_o) \qquad \ldots (5.5)$$

Use of this parameter of course implies that the motion is sinusoidal, which is, in general, a very crude approximation, but it will suffice for an order of magnitude estimation.

Now from (5.1)

$$K_s = -2\alpha c_1 \qquad \ldots(5.6)$$

and so

$$\overline{K}/|K_s| = \frac{\beta I}{2\alpha} \left[ \frac{\sinh c_1 x_o}{c_1 x_o} - \frac{\sinh 2c_1 x_o}{2c_1 x_o} \right] \qquad \ldots(5.7)$$

If the measured value of $\overline{K}$ (i.e., the square of the measured angular frequency of oscillation) is plotted against I, the intercept of the resulting line with the $\overline{K}$ axis will thus give the correct value of $K_s$ if the oscillations are sufficiently small, but in general it will be in error in the ratio $(\sinh 2c_1 x_o)/2c_1 x_o$.

This expression is plotted in Figure 14 as a function of $x_o$. It is clear that the amplitude of the oscillations must be kept below about 0.25 cm if this technique is to give a reasonable accuracy.

The implication of this result is that some form of displacement detector is a prerequisite for determination of the inherent spring constant, as visual observation of the test-mass did not allow sufficiently accurate estimation of the oscillation amplitude.

## 5.3 Experimental Results

In order to make the measurement described above, a simple optical displacement detector was constructed and attached to the dewar. Details of this device will not be given here, as it is described fully in Reference 8. The output characteristic is shown in Figure 15; the linear range was approximately 1 mm. The axial position of the null inside

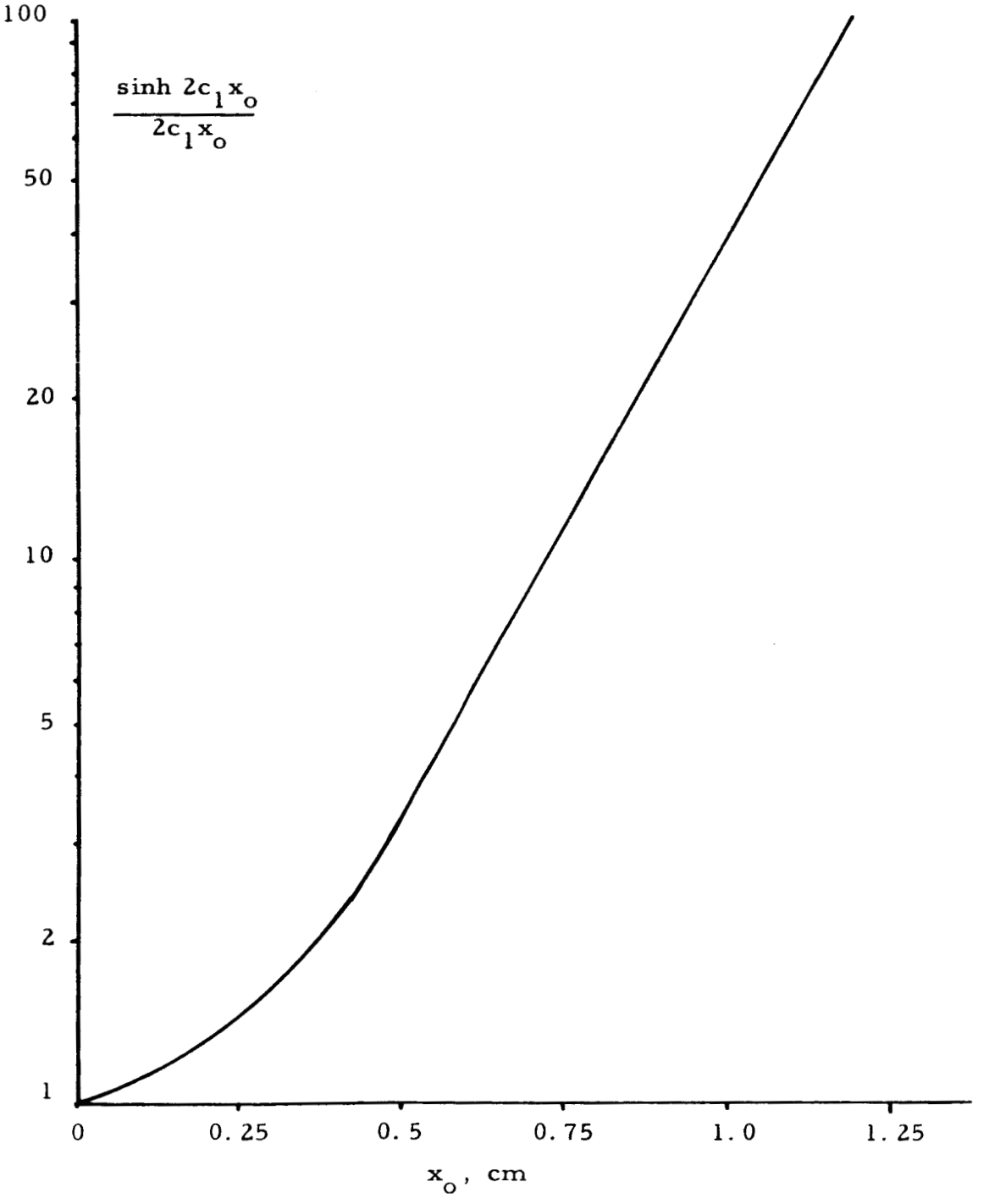


Figure 14: Effect of Oscillation Amplitude on Accuracy of Spring-Constant Measurement

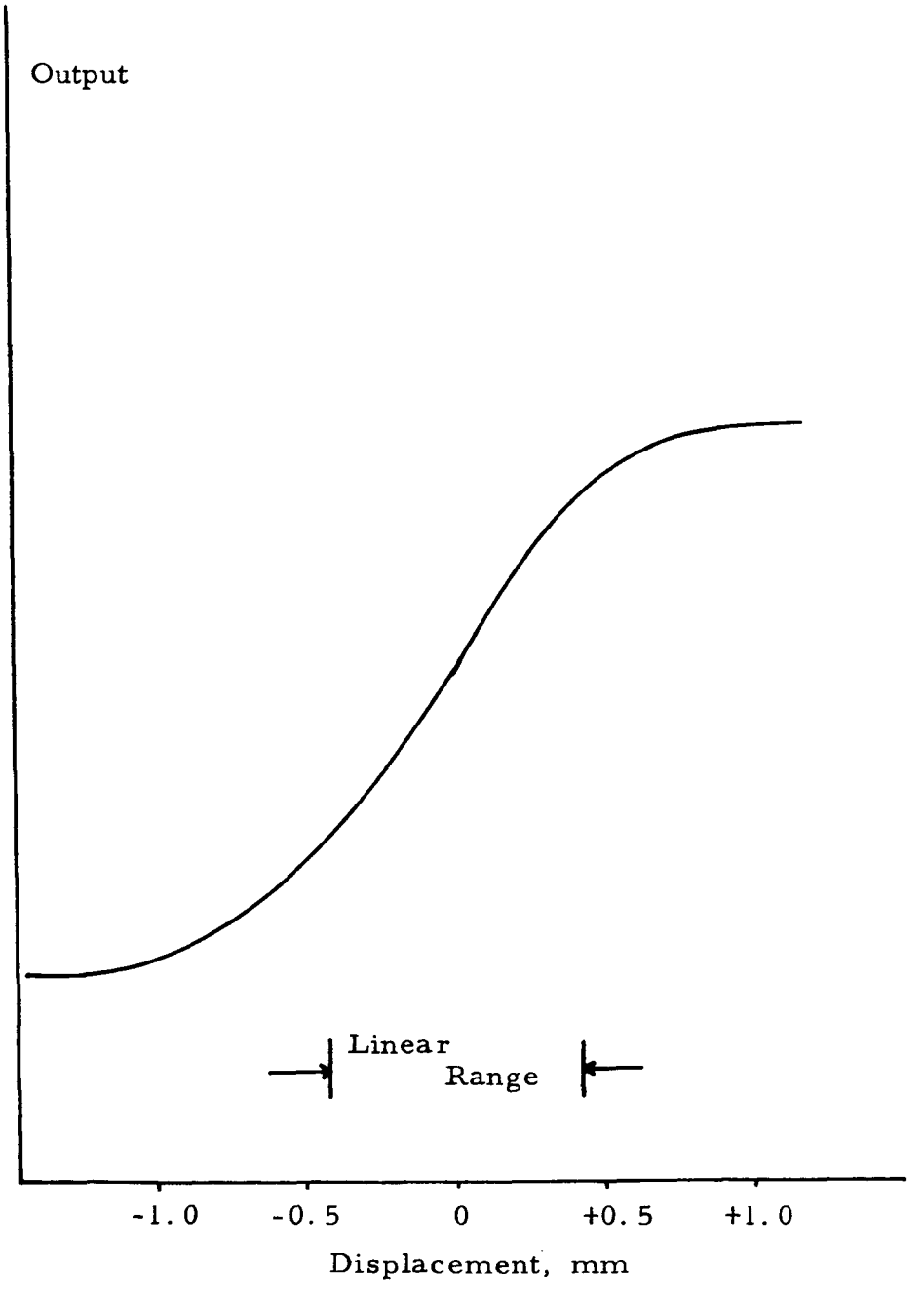


Figure 15: Displacement Detector Output Characteristic

the suspension was determined by the location of a small prism assembly mounted inside the copper tube.

The prisms were moved until the output null was as close to the center of the superconducting tube as possible. The stabilization coils were fixed in position near the ends of the suspension: when the magnet was inserted, it was found that a coil current of 11 mA was the minimum for stability. The levelling of the base of the dewar was then adjusted, causing the magnet to move into the linear range of the detector, until an output close to null was obtained.

The test mass was displaced to one end of the linear range by bringing an external magnet near one of the dewar windows and then released. The output of the detector due to the resultant damped axial oscillation was recorded, and the experiment repeated for several different values of the coil current. A typical record is shown in Figure 16.

The first parameter that could be determined from these tests is the damping due to eddy current generation in the copper tube. The amplitudes of successive cycles of the oscillations are plotted in Figure 17 as functions of the time. The time constant was found to be approximately 3 seconds.

Secondly, the spring constant corresponding to each record (i.e., $m\omega^2$) was computed and plotted as a function of the coil current, as shown in Figure 18. The inherent suspension spring constant was found to be approximately -15 dynes/cm.

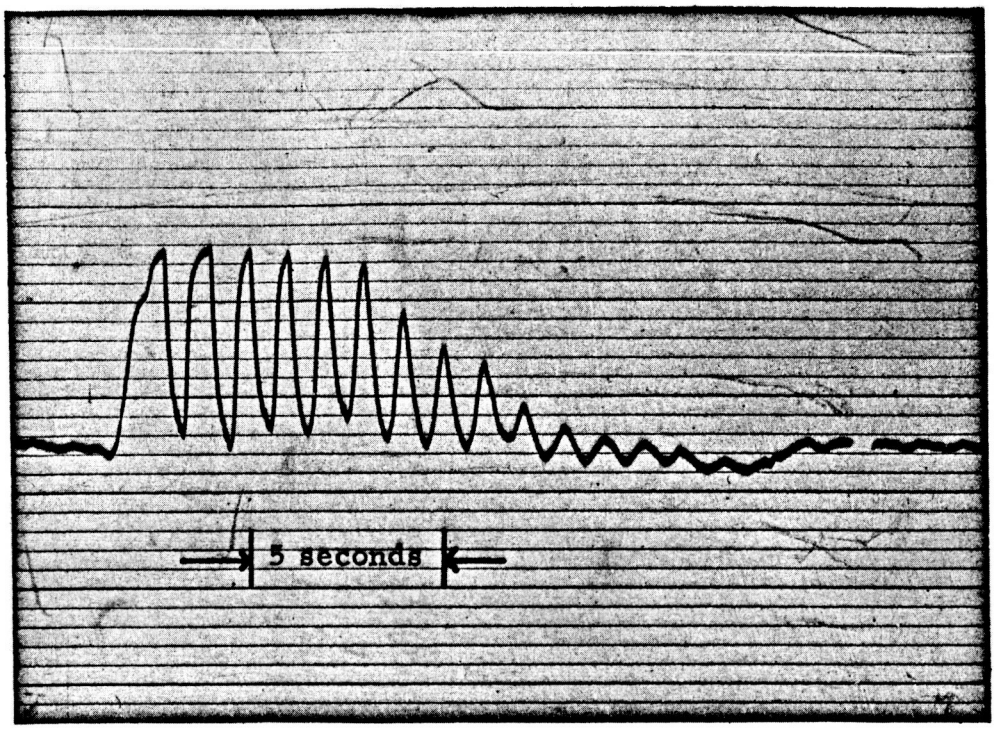


Figure 16: A Typical Test Record

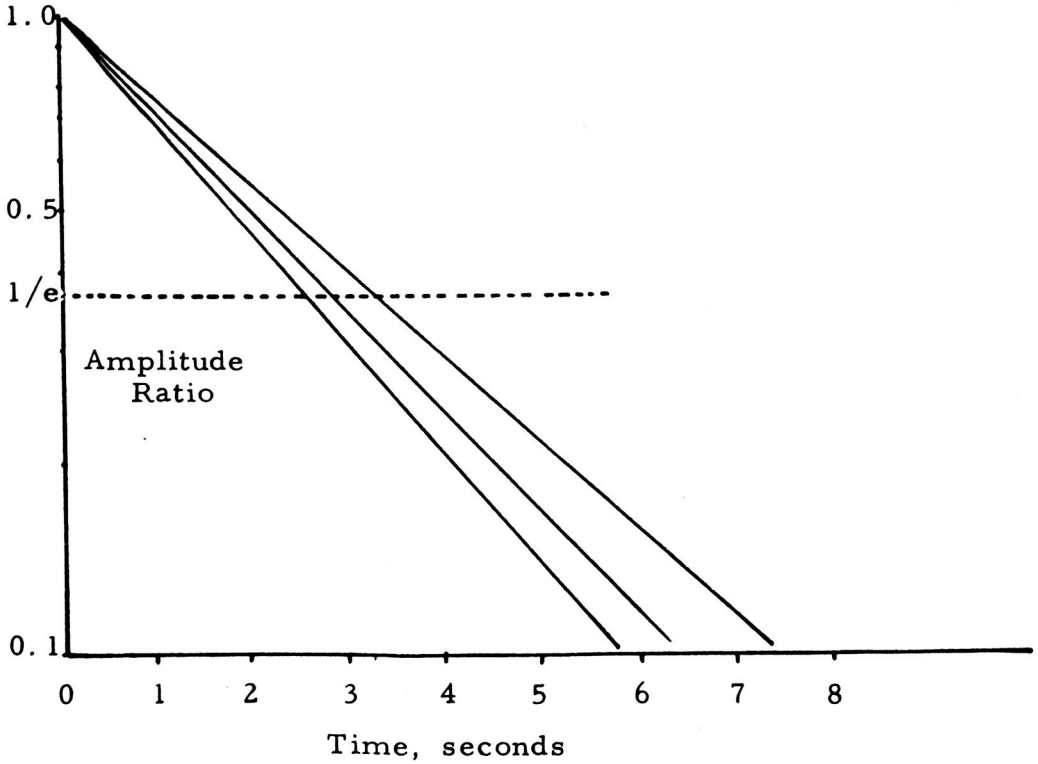


Figure 17: Damping of Axial Oscillation

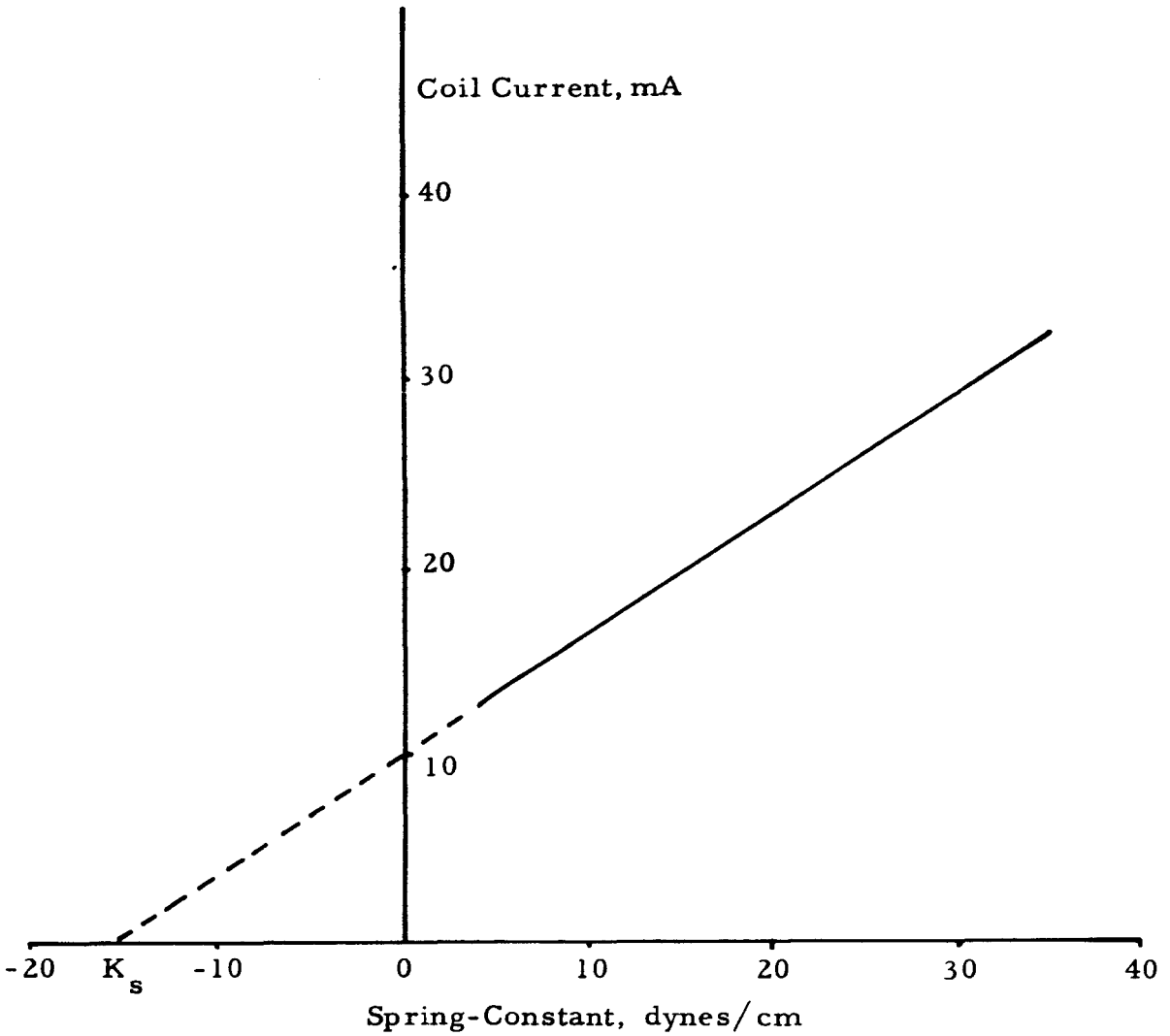


Figure 18: Suspension Axial Spring Constant vs. Coil Current

From Eqs. (5.6) and (5.2), the values of the constants in Eq. (5.1) are

$$\alpha \cong 2.5 \text{ dynes}$$
$$\beta \cong 0.5 \text{ dynes/mA} \qquad \ldots (5.8)$$

Two more simple tests were performed as an aid in evaluating the suspension. In the first of these, the base of the dewar was suddenly tilted through 12 arc seconds, with a current of 15 mA flowing in the coils. It was found that this produced a very easily observable change in the detector output, as shown in the record of Figure 19. The record was to some extent corrupted by noise due to shaking of the test fixture, but it was estimated that a tilt of 2 arc seconds, corresponding to $10^{-5}$g, would be well above the threshold, even without the rest of the LLAMA system.

As a check on this result, the current in one of the coils was increased suddenly, when the magnet was floating near null. From Eq. (A.36), the force on the magnet due to a step $\Delta I$ in <u>one</u> of the coils is $\frac{\beta}{2}\Delta I$: it was found that a change of 0.05 mA was readily observable, corresponding to a force of 0.013 dynes, equivalent to $12.10^{-6}$g. The agreement with the preceding result was surprisingly good.

The results of the tests are tabulated in Table 5.1, for ready reference.

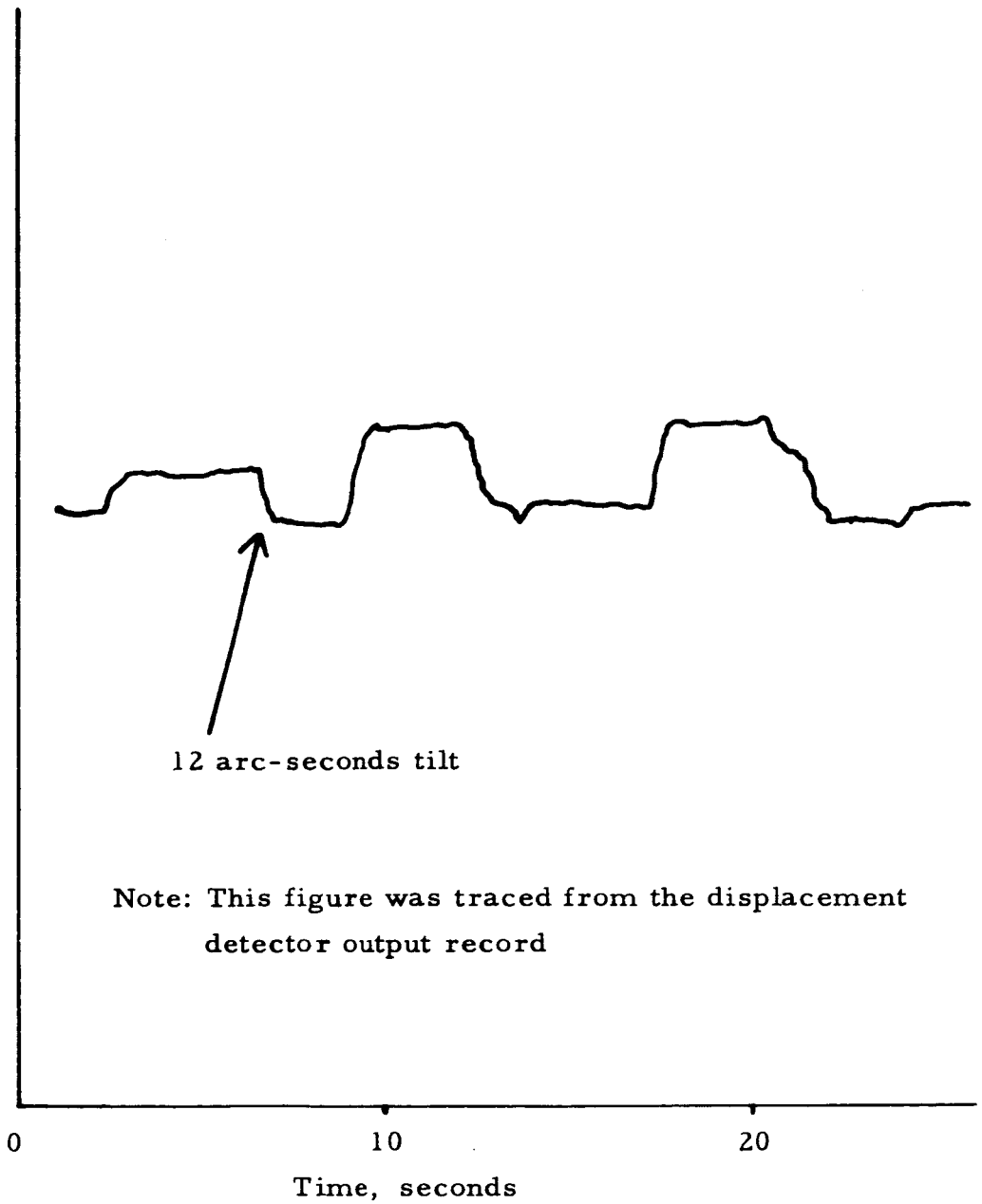


Figure 19: Response to Steps in Input Acceleration

| | |
|---|---|
| Initial inherent suspension spring constant ($K_s$) | -15 dynes/cm |
| Force constant of suspension ($\alpha$) | 2.5 dynes |
| Force constant of stabilizing coils ($\beta$) | 0.5 dynes/mA |
| Natural axial damping time constant | 3 seconds |
| Threshold as an elementary accelerometer | $10^{-5}$ g |

Table 5.1: Characteristics of Experimental Suspension

## 5.4 Interpretation of Test Results

The observed initial spring constant, $K_s$, is of the same order as that which would be obtained if the magnet were placed in free space between two vertical soft iron plates, separated by the length of the LLAMA suspension. It is considered that the numerical value observed does not have great general significance, as it is undoubtedly greatly affected by the width of the slit along the top of the suspension. However, the observed conditions for stability do lend some support to the belief that the displacement dependence of the axial forces does follow the hyperbolic form derived in the Appendix.

In any case, the end-effect compensation coils performed extremely well, as evidenced by the low acceleration threshold when the suspension was used as an elementary accelerometer. It is quite surprising that the present instrument, which was designed for checking feasibility, not for high performance, should do so well, without any of the other components of LLAMA.

It is also clear that the present suspension incorporates a very useful amount of damping, which should make it a relatively simple matter to close the restoring force feedback loop. This expectation has been borne out in practice[8].

## 5.5 Conclusions: Implications for Future Work

At the present stage of development, LLAMA has shown considerable promise of exceptional sensitivity. There is little doubt that the value of the measured acceleration threshold is determined by the limitations of the present displacement detector and the stability of the test fixture rather than by the suspension itself. It is expected that use of the interferometer and creation of a more stable environment by mounting the instrument on a suitable seismic pier would enable the threshold to be lowered by several orders of magnitude, even without improving the rather primitive arrangement of the superconductor.

As far as the suspension is concerned, the main task for the future is modification of the design in an attempt to approach the theoretical performance limits. In the first place, the sheet of niobium will be replaced by a niobium film vacuum-deposited on the outside of a finely-lapped copper tube, thereby minimising distortion of the superconducting surface. The necessary slit will be produced by scribing a line along the top of the tube, of the minimum width which will guarantee prevention of supercurrents across the barrier.

Two other possible improvements which will be investigated are:

i) Leaving narrow bridges of superconductor across the slit at either ends of the tube, to give a multiply-connected suspension in which the net flux through the slit (and through the ends of the tube) is held constant at the value which existed at the time of transition of the superconductor. It is expected that this will reduce the end effects.

ii) Forming the outside of the cylinder to a slightly bulbous shape before deposition of the niobium. Determination of the optimum shape will probably require a computer study of the perturbed field equations, together with extensive experimentation, but, at least in theory, it is possible to eliminate the end effects completely by this technique.

If all else fails, the performance can be improved by simply using a longer suspension, although this would require a larger dewar.

Finally, it is recognized that the cryogenic requirements of the LLAMA suspension, which are acceptable in the laboratory environment, would cause considerable difficulty in deploying the system for any length of time on a space mission, where many of the most interesting applications of low-level accelerometry occur. Fortunately, the support forces required in space are generally much lower than in the terrestrial case, so that a suspension using other diamagnetic materials than superconductors may be feasible. In particular, a thick-walled bismuth tube, of the same internal diameter as the present suspension, would support the LLAMA test mass in a transverse field of at least $10^{-4}$ g . This figure could be improved by using a smaller diameter tube and a more powerful magnet, such as a platinum-cobalt alloy rather than Alnico V.

# APPENDIX

## THE FIELD INSIDE THE LLAMA SUSPENSION

### A. 1 Introduction

The purpose of this Appendix is to derive expressions for the field inside several mathematical models which represent in some sense the LLAMA Meissner effect test-mass suspension. Because of the rather highly idealized nature of the models used, the results can be applied to the present suspension only with considerable caution. However, they are useful in the discussion of ultimate performance limitations in Chapter III, and again in the interpretation of the test results in Chapter V.

### A. 2 A Suspension of Infinite Length

The simplest case to be considered is that of a magnet which is stationary on the axis of a superconducting cylinder of infinite length (the steady-state case in free fall). The effects of the slit along the top of the suspension are ignored.

In this static situation, the magnetic field $\underline{H}$ may be set equal to the negative gradient of a scalar potential $\Omega$. For the region internal to the tube but external to the magnet, $\Omega$ is a solution of Laplace's equation

$$\nabla^2 \Omega = 0 \qquad \ldots (A.1)$$

subject to the applicable boundary conditions.

Set up a circular cylindrical coordinate system r, $\theta$, z with the z-axis along the axis of the cylinder. Since by symmetry there is no variation of $\Omega$ with $\theta$, the above equation becomes

$$\frac{1}{r}\frac{\partial}{\partial r}\left(r\frac{\partial \Omega}{\partial r}\right) + \frac{\partial^2 \Omega}{\partial z^2} = 0 \qquad \ldots (A.2)$$

which may be solved by the standard separation of variables technique. Putting

$$\Omega = R(r)\, Z(z) \qquad \ldots (A.3)$$

the pair of equations

$$\frac{1}{r}\frac{d}{dr}\left(r\frac{dR}{dr}\right) + k^2 R = 0 \qquad \ldots (A.4a)$$

and

$$\frac{d^2 Z}{dz^2} - k^2 Z = 0 \qquad \ldots (A.4b)$$

are obtained, where $k^2$ is the separation constant.

Eq. (A.4a) is a Bessel equation, and (A.4b) gives trigonometric or hyperbolic solutions, depending on whether k is imaginary or real. In order to specify the solutions further, it is necessary to consider the boundary conditions.

At the superconducting surface, because the magnetic field

cannot penetrate and because there are no magnetic poles there, the normal component of the field is

$$H_r = - \frac{\partial \Omega}{\partial r} = 0 \qquad \ldots (A.5)$$

so that homogeneous Neumann boundary conditions obtain on the curved surface of the cylinder.

As the tube is of infinite length, the boundary condition at the ends is of course that $\Omega$ be zero there.

Strictly speaking, the source of the field is the magnetostatic potential distribution over the surface of the magnet. Eq. (A. 1) should be solved by finding the Green's function corresponding to a source point $\underline{r}_o$ on the surface of the magnet, weighting this with the potential distribution, and integrating in the source coordinates over the magnet. However, since the diameter of the magnet is very much less than the diameter of the tube, an adequate approximation is obtained if the magnet be idealized so that it consists of a pair of poles, of strength $\pm p$ at $(0, 0, \pm d)$. The Green's function is then a solution of

$$\nabla^2 G = -4\pi\delta \qquad \ldots (A.6)$$

where $\delta$ is a 'volume' delta function at one of the poles (i. e., the volume integral of $\delta$ is unity). Note that Gaussian units are employed in this equation.

The choice of a form for the trial solution of this equation is guided by the following considerations:

i) As z has an infinite range, and since $\Omega$ is continuous and has a finite mean value, a Fourier integral representation of the z-dependence is appropriate.

ii) Because of the radial symmetry, only zero-order cylindrical harmonics are required. In addition, since $\Omega$ must be finite on the z-axis, only Bessel functions of the first kind will appear.

The trial solution is therefore

$$G = \sum_s J_o(c_s r) \int_{-\infty}^{\infty} A_s(k)\, e^{-jkz}\, dk \qquad \ldots (A.7)$$

where, if a is the radius of the tube, $c_s a$ is the $s^{th}$ root of the equation

$$\frac{d}{d\lambda} J_o(\lambda) = 0 \qquad \ldots (A.8)$$

thus satisfying the required Neumann conditions at the superconductor.

Inserting (A. 7) in (A. 6) and carrying out the indicated differentiation gives

$$\sum_s J_o(c_s r) \int_{-\infty}^{\infty} (k^2 + c_s^2)\, A_s(k)\, e^{-jkz} dk = 4\pi\delta \qquad \ldots (A.9)$$

which may be solved for $A_s(k)$ by making use of the properties of the Fourier transform and the orthogonality of the Bessel functions. Multiplying both sides of (A. 9) by $J_o(c_s r)\, e^{jkz}$ and integrating over the volume of the cylinder gives the result

$$2\pi^2 a^2 J_o^2(c_s a)\,(k^2+c_s^2)\,A_s(k) = 4\pi e^{jkd} \qquad \ldots (A.10)$$

where the delta function has been taken at the positive pole. Eq. (A.7) then gives

$$G = \frac{2}{\pi a^2} \sum_s \frac{J_o(c_s r)}{J_o^2(c_s a)} \int_{-\infty}^{\infty} \frac{e^{-jk(z-d)}}{(k^2+c_s^2)}\, dk \qquad \ldots (A.11)$$

The integral is readily evaluated as $\frac{\pi}{c_s} \exp(-c_s|z-d|)$.

Thus

$$G = \frac{2}{a} \sum_s \frac{J_o(c_s r)}{c_s a J_o^2(c_s a)} \exp(-c_s|z-d|) \qquad \ldots (A.12)$$

The potential $\Omega$ is obtained by summation of the Green's functions corresponding to the two poles, weighted by the pole strengths. Thus

$$\Omega = \pm \frac{4p}{a} \sum_{s=1}^{\infty} \frac{J_o(c_s r)}{c_s a J_o^2(c_s a)}\, e^{-c_s|z|} \sinh c_s d \qquad \ldots (A.13)$$

for $|z| > d$, where the positive sign is to be used when the nearest pole is positive, and conversely.

## A. 3 A Finite-Length Case

The purpose here is to find the way in which the potential distribution of Eq. (A. 13) is modified when the tube is of finite length, and hence to develop an approximate expression for the axial force on the test-mass due to end effects.

In order to solve Laplace's equation for this case, it is of course necessary to assign definite boundary conditions at the ends of the tube. If homogeneous Neumann conditions are chosen (e. g., plane superconducting ends) a configuration results which is clearly stable with respect to all displacements of the test-mass from the center. Conversely, homogeneous Dirichlet conditions (e. g., plane high permeability ends connected by an external low-reluctance path) produce an axially unstable situation.

The actual end boundary conditions lie somewhere between these extremes, but their precise nature is unknown. Since the real suspension is unstable, the best approximation available is that of a tube with Dirichlet ends. This is not too unreasonable, because the lines of force are parallel to the axis of the tube at the superconducting surface and close to the axis, so that the field emerging from the ends should be largely perpendicular to the ends, as required by Dirichlet conditions.

Since the forces due to end effects are not expected to depend very strongly on the precise height at which the magnet is floating, it is again assumed to be on the axis of the tube.

A circular cylindrical coordinate system $r, \theta, z$ is set up, with the origin at the center of the tube. The magnet is again idealized so

that it consists of a pair of poles of strength $\pm p$, located at $(0, 0, x \pm d)$, where x is the axial displacement of the center of the magnet.

The development is similar to that in the preceding Section, except that a Fourier series, rather than integral, representation of the z-dependence is now appropriate. The trial solution of (A. 6) is therefore now taken as

$$G = \sum_{k,\,s} A_{ks}\, J_o(c_s r)\, \sin\left(\frac{k\pi}{2L}(z+L)\right) \qquad \ldots (A.\,14)$$

which goes to zero at $z = \pm L$, the ends of the tube, and satisfies homogeneous Neumann conditions at the curved surface.

Inserting this expression in (A. 6) gives the result

$$\sum_{k,\,s} \left(\left(\frac{k\pi}{2L}\right)^2 + c_s^2\right) A_{ks}\, J_o(c_s r)\, \sin\left(\frac{k\pi}{2L}(z+L)\right) = 4\pi\delta \qquad \ldots (A.\,15)$$

This equation is now multiplied by $J_o(c_s r)\, \sin\left(\frac{k\pi}{2L}(z+L)\right)$ and integrated over the volume of the cylinder, to obtain

$$\pi L a^2 J_o^2(c_s a)\, \left(\left(\frac{k\pi}{2L}\right)^2 + c_s^2\right) A_{ks} = 4\pi \sin\left(\frac{k\pi}{2L}(x+d+L)\right)$$

$$\ldots (A.\,16)$$

where the delta function has been taken at the positive pole. Then

$$G = \frac{4}{La^2} \sum_s \frac{J_o(c_s r)}{J_o^2(c_s a)} \sum_{k=o}^{\infty} \frac{\sin\left(\frac{k\pi}{2L}(x+d+L)\right) \sin\left(\frac{k\pi}{2L}(z+L)\right)}{\left(\frac{k\pi}{2L}\right)^2 + c_s^2}$$

$$\ldots (A.\,17)$$

As before, the magnetostatic potential is found by taking the

weighted sum of the Green's functions corresponding to the two poles. Using the trigonometric identity

$$\sin\left(\frac{k\pi}{2L}(x+L+d)\right) - \sin\left(\frac{k\pi}{2L}(x+L-d)\right)$$

$$= 2\cos\left(\frac{k\pi}{2L}(x+L)\right)\sin\frac{k\pi d}{2L} \qquad \ldots (A.18)$$

the potential is found to be

$$\Omega = \frac{4p}{La^2}\sum_s \frac{J_o(c_s r)}{J_o^2(c_s a)} \sum_{k=-\infty}^{\infty} \frac{\sin\left(\frac{k\pi}{2L}(z+L)\right)\cos\left(\frac{k\pi}{2L}(x+L)\right)\sin\frac{k\pi d}{2L}}{\left(\frac{k\pi}{2L}\right)^2 + c_s^2}$$

$\ldots (A.19)$

where the sum over k has been extended to $-\infty$ by virtue of the evenness of the terms with respect to k.

It is possible, although somewhat involved, to obtain a closed form representation of the z-dependence. To simplify the algebra, the products of trigonometric functions are first expanded:

$$\sin\left(\frac{k\pi}{2L}(z+L)\right)\cos\left(\frac{k\pi}{2L}(x+L)\right)\sin\frac{k\pi d}{2L}$$

$$= \frac{1}{2}\left[\sin\left(\frac{k\pi}{2L}(2L+x+z)\right) + \sin\left(\frac{k\pi}{2L}(z-x)\right)\right]\sin\frac{k\pi d}{2L}$$

$$= \frac{1}{4}\left[\cos\left(\frac{k\pi}{2L}(2L+x+z-d)\right) - \cos\left(\frac{k\pi}{2L}(2L+x+z+d)\right)\right.$$

$$\left. + \cos\left(\frac{k\pi}{2L}(z-x-d)\right) - \cos\left(\frac{k\pi}{2L}(z-x+d)\right)\right]$$

$\ldots (A.20)$

The problem has therefore been reduced to evaluating sums of the form

$$S = \sum_{k=-\infty}^{\infty} \frac{\cos \frac{k\pi q}{2L}}{(\frac{k\pi}{2L})^2 + c_s^2} \qquad \ldots (A.21)$$

which may be achieved by use of Poisson's sum formula[19]:

$$\sum_{n=-\infty}^{\infty} f(\lambda n) = \frac{\sqrt{(2\pi)}}{\lambda} \sum_{m=-\infty}^{\infty} \Phi(\frac{2m\pi}{\lambda}) \qquad \ldots (A.22)$$

where $\Phi$ is the Fourier transform of f.

For the present application, put

$$f(n) = \frac{\cos nq}{n^2 + c_s^2} \qquad \ldots (A.23)$$

and

$$\lambda = \frac{\pi}{2L} \qquad \ldots (A.24)$$

Then

$$\Phi(\omega) = \frac{1}{\sqrt{2\pi}} \int_{-\infty}^{\infty} \frac{e^{j\omega n} \cos nq}{n^2 + c_s^2} \, dn$$

$$= \frac{\sqrt{\pi}}{2c_s\sqrt{2}} \left( e^{-c_s|\omega+x|} + e^{-c_s|\omega-x|} \right) \qquad \ldots (A.25)$$

so

$$\sum_n f(\lambda n) = \frac{L}{c_s} \sum_m \left( e^{-c_s|4Lm+q|} + e^{-c_s|4Lm-q|} \right) \qquad \ldots (A.26)$$

An examination of (A. 20) shows that, for all the sums of interest, $|q| < 4L$. Thus

$$\sum_{n=-\infty}^{\infty} f(\lambda n) = \frac{2L}{c_s} \left( e^{-c_s|q|} + 2\cosh c_s q \sum_{m=1}^{\infty} e^{-4c_s Lm} \right)$$

$$= \frac{2L}{c_s} \left( e^{-c_s|q|} + 2\cosh c_s q \, \frac{e^{-4c_s L}}{1-e^{-4c_s L}} \right)$$

$$= \frac{2L}{c_s} \, \frac{\cosh c_s (|q|-2L)}{\sinh 2c_s L} \qquad \ldots (A.\ 27)$$

Substituting the various values of q from (A. 20) and inserting the results in (A. 19) gives the following expressions for the potential, after some algebraic reduction:

$$\Omega = \frac{8p}{a} \sum_s \frac{J_o(c_s r) \sinh c_s d \sinh c_s (L-z) \cosh c_s (L+x)}{c_s a \, J_o^2(c_s a) \sinh 2c_s L}$$

$\ldots (A.\ 28a)$

for $z > x+d$ and

$$\Omega = -\frac{8p}{a} \sum_s \frac{J_o(c_s r) \sinh c_s d \sinh c_s (L+z) \cosh c_s (L-x)}{c_s a \, J_o^2(c_s a) \sinh 2c_s L}$$

$\ldots (A.\ 28b)$

for $z < x-d$

As a check on the algebra, note that (A. 28a) is zero at z=L and (A. 28b) at z=-L. Also, both expressions have the limiting form

$$\Omega = \pm \frac{4p}{a} \sum_s \frac{J_o(c_s r)}{c_s a \, J_o^2(c_s a)} e^{-c_s|z-x|} \sinh c_s d \qquad \ldots (A.\ 29)$$

as L approaches infinity, which is the correct value.

If $L \gg a$, and the magnet is not near one of the ends of the tube, it is clear from Eqs. (A. 28) that only the first term in the sums over s will be significant.

At the ends of the tube, the magnetic field of course has only a z-component. The net force on the end at z=L is given by

$$F_1 = \frac{1}{8\pi} \int_S H_z^2 \, dS \qquad \ldots (A.30)$$

where S is the area of the end. From (A. 28a)

$$F_1 = \frac{-8p^2}{a^2 J_o^2(c_1 a)} \quad \frac{\sinh^2 c_1 d \ \cosh^2 c_1 (L+x)}{\sinh^2 2c_1 L} \qquad \ldots (A.31)$$

Similarly, the force on the other end is

$$F_2 = \frac{8p^2}{a^2 J_o^2(c_1 a)} \quad \frac{\sinh^2 c_1 d \ \cosh^2 c_1 (L-x)}{\sinh^2 2c_1 L} \qquad \ldots (A.32)$$

The net force on the magnet is of course the negative difference of these forces, or

$$F = \frac{8p^2}{a^2 J_o^2(c_1 a)} \quad \frac{\sinh^2 c_1 d}{\sinh 2c_1 L} \quad \sinh 2c_1 x \qquad \ldots (A.33)$$

## A. 4 Forces from Stabilizing Coils

Consider the infinite length tube of Section A. 2, with the addition of single-turn coils of radius b at $z = \pm z_c$. The axes of the coils are coincident with the tube axis. With a current of I amperes flowing in one of the coils, the force on an element $\underline{dl}$ of it is given by

$$\underline{dF} = 10 \; I \, \underline{dl} \times \underline{H} \qquad \ldots (A.34)$$

where $\underline{dl}$ is measured in cm and $\underline{H}$ is the magnetic field of the test-mass in oersteds.

By symmetry, radial forces will cancel, so the net force on the coil is in the axial direction:

$$F_z = 20\pi \; I \, b \, H_r \qquad \ldots (A.35)$$

Assuming $(z_c - x)$ is fairly large (at least of the order of the tube radius), $H_r$ may be calculated from (A. 13) or (A. 33), retaining only the first term of the sum. Thus

$$F_z = \mp \frac{80\pi \, b \, p}{a^2 J_o^2(c_1 a)} \; J_1(c_1 b) \sinh c_1 d \;\; I \; e^{-c_1 |z_c - x|} \qquad \ldots (A.36)$$

If the same current is flowing in each coil, the net force on the magnet is

$$F_c = \frac{160\pi \, b \, p}{a^2 J_o^2(c_1 a)} \; J_1(c_1 b) \sinh c_1 d \;\; e^{-c_1 |z_c|} \; I \; \sinh c_1 x \qquad \ldots (A.37)$$

# REFERENCES


1) Brune, J. N., and Oliver, J.: 'The Seismic Noise of the Earth's Surface', Bulletin of the Seismological Society of America, Vol. 49, #4, Oct. 1959, pp 349-353.

2) Roberson, R. E.: 'Attitude Control of Satellites and Space Vehicles', in Advances in Space Science, Vol. 2, pp 351-436, Academic Press, NY, 1960.

3) Weber, J.: General Relativity and Gravitational Waves, Interscience Tracts on Physics and Astronomy, #10, 1961; Sec. 8.2, p 126.

4) Tilton, Parkin, Covert, Coffin and Chrisinger: 'The Design and Initial Operation of a Magnetic Model Suspension and Force Measurement System', M. I. T. Aerophysics Lab. Technical Report #22, August, 1962.

5) Gilinson, P. J., Jr., Denhard, W. G. and Frazier, R. H.: 'A Magnetic Support for Floated Inertial Instruments', M. I. T. Instrumentation Lab. Report R-277, April, 1960.

6) Nordsieck: 'Principles of the Electric Vacuum Gyroscope', in Progress in Astronautics and Rocketry, Vol. 8: Guidance and Control, p 435; Academic Press, NY, 1962.

7) Martin Company, Orlando, Florida: Report OR 3673, 'Analytical Report on Particle Reference Device'.

8) Ezekiel, S.: Master of Science Thesis, M. I. T Department of Aeronautics and Astronautics, June, 1964.

9) Kamerlingh-Onnes, H: 'Disappearance of the Electrical Resistance of Mercury at Helium Temperatures', Commun. Phys. Lab. Univ. Leiden, #122b (1911); ibid, Supplement #34 (1913).

10) Quinn, D. J., III, and Ittner, W., III: 'Resistance in a Superconductor', J. Appl. Phys., Vol. 33, 1962, p 748.

11) Bremer, J. W.: Superconductive Devices, McGraw-Hill, N. Y., 1962, p 3.

12) Schawlow, A. L.: Phys. Rev., Vol. 101, 1956, p 573

13) Meissner, W. and Ochsenfeld, R.: 'Ein Neuer Effekt bei Eintritt

der Supraleitfahigkeit', Naturwissenschaften, Vol. 21, 1933, p 787.
14) London, F., and London, H.: Proc. Roy. Soc. A, Vol. 149, 1935, p 71.
15) Bardeen, J., Cooper, L. N., and Schrieffer, J. R.: Phys. Rev., Vol. 106, 1957, p 162; ibid, Vol. 108, 1957, p 1175.
16) Arkadiev, V.: Nature, Vol. 160, 1947, p 330.
17) Harding, J. T. and Tuffins, R. H., in Advances in Cryogenic Engineering (K. D. Timmerhaus, Ed.), Plenum Press, NY, 1961, Vol. 6, p 95.
18) Simon, I: J. Appl. Phys., Vol. 24, 1955, p 19.
19) Morse, P. M. and Feshbach, H.: Methods of Theoretical Physics, McGraw-Hill, NY, 1953, p 494.